

Locating the boundaries of Pareto fronts: A Many-Objective Evolutionary Algorithm Based on Corner Solution Search

Xinye Cai, Haoran Sun, Chunyang Zhu, Zhenyu Li, Qingfu Zhang

Abstract—In this paper, an evolutionary many-objective optimization algorithm based on corner solution search (MaOEA-CS) was proposed. MaOEA-CS implicitly contains two phases: the exploitative search for the most important boundary optimal solutions – corner solutions, at the first phase, and the use of angle-based selection [1] with the explorative search for the extension of PF approximation at the second phase. Due to its high efficiency and robustness to the shapes of PFs, it has won the CEC'2017 Competition on Evolutionary Many-Objective Optimization. In addition, MaOEA-CS has also been applied on two real-world engineering optimization problems with very irregular PFs. The experimental results show that MaOEA-CS outperforms other six state-of-the-art compared algorithms, which indicates it has the ability to handle real-world complex optimization problems with irregular PFs.

Index Terms—Corner solution; boundary optimal solution; explorative search; exploitative search; many-objective optimization;

I. INTRODUCTION

A multiobjective optimization problem (MOP) can be defined as follows:

$$\begin{aligned} &\text{minimize} && F(x) = (f_1(x), \dots, f_m(x))^T \\ &\text{subject to} && x \in \Omega \end{aligned} \quad (1)$$

where Ω is the *decision space*, $F : \Omega \rightarrow R^m$ consists of m real-valued objective functions. The *attainable objective set* is $\{F(x)|x \in \Omega\}$. Let $u, v \in R^m$, u is said to *dominate* v , denoted by $u \prec v$, if and only if $u_i \leq v_i$ for every $i \in \{1, \dots, m\}$ and $u_j < v_j$ for at least one index $j \in \{1, \dots, m\}$ ¹. A solution $x^* \in \Omega$ is *Pareto-optimal* to (1) if there exists no solution $x \in \Omega$ such that $F(x)$ dominates $F(x^*)$. The set of all the Pareto-optimal points is called the *Pareto set (PS)* and the set of all the Pareto-optimal objective

vectors is the *Pareto front (PF)* [2]. MOPs with more than three objectives are commonly referred to as many-objective optimization problems (MaOPs).

Over the past decades, multi-objective evolutionary algorithms (MOEAs) have been recognized as a major methodology to approximate PFs in MOPs [3]–[8]. However, most MOEAs are designed to address MOPs with two or three objectives. It is well-known that the performance of MOEAs, especially Pareto-dominance based MOEAs, deteriorate when dealing with MaOPs with more than three objectives. Generally speaking, MaOPs are very challenging due to the following reasons [9], [10].

- 1) With the increase of the number of objectives, the selection pressure of Pareto dominance-based MOEAs deteriorates rapidly, as most solutions become nondominated to each other [11]–[14]. For example, Pareto dominance-based MOEAs such as NSGA-II [5] and SPEA2 [15] can not perform well on MaOPs.
- 2) The PF of an m -objective non-degenerate MOP (or MaOP) is an $(m - 1)$ -dimensional manifold [16], [17] (PFs of degenerate MOPs (or MaOPs) are less than $(m - 1)$ -dimensional). This indicates that maintaining diversity with a limited number of solutions for MaOPs become more and more difficult. A good example is that the diversity maintenance method used in MOEAs, such as the crowding distance in NSGA-II [5] has become ineffective for MaOPs.

Over the recent years, a large number of many objective optimization evolutionary algorithms (MaOEA) have been proposed to address MaOPs [18]–[25]. Based on the selection of solutions, they can be roughly divided to following four categories.

- 1) Modified-Pareto-dominance-based approaches directly modify the Pareto-dominance relation to further enhance the selection pressure towards PFs for MaOPs. ϵ -dominance [26], [27], grid-dominance [28], volume-dominance [29], and subspace-dominance [30], [31] belong to this type of approaches.
- 2) Diversity-based approaches further enhance the selection pressure of MOEAs by maintaining better diversity. For instance, a diversity management mechanism based on the spread of the population was introduced in [32]. A shift-based density estimation (SDE) was proposed as a diversity maintenance scheme to further enhance the selection pressure in [33].

This paper is submitted for possible publication. Reviewers can use this manuscript as an alternative in peer review.

Xinye Cai, Haoran Sun, Chunyang Zhu and Zhenyu Li are with the College of Computer Science and Technology, Nanjing University of Aeronautics and Astronautics, Nanjing, Jiangsu, 210016 P. R. China; and also with the Collaborative Innovation Center of Novel Software Technology and Industrialization, Nanjing 210023, China (e-mail: xinye@nuaa.edu.cn, nuaa_sunhr@yeah.net).

Qingfu Zhang is with the Department of Computer Science, City University of Hong Kong, Kowloon, Hong Kong SAR (e-mail: qingfu.zhang@cityu.edu.hk).

This work was supported in part by the National Natural Science Foundation of China (NSFC) under grant 61300159, by ANR/RGC Joint Research Scheme under grant A-CITYU101/16, by the Natural Science Foundation of Jiangsu Province of China under grant BK20130808 and by China Postdoctoral Science Foundation under grant 2015M571751.

¹In the case of maximization, the inequality signs should be reversed.

- 3) Indicator-based approaches adopt the indicator metric as the selection criteria. For example, hypervolume [34] is a well-known indicator, which considers both convergence and diversity. In [35], a S -metric selection by maximizing the hypervolume of the solution sets was proposed. To further reduce the computational complexity of calculating hypervolume, Bader et al. proposed a hypervolume estimation algorithm (HypE) [18], where, instead of calculating the exact values of hypervolume, Monte Carlo sampling is adopted to approximate it.
- 4) Decomposition-based approaches decomposes a multi-objective optimization problem into a number of subproblems by linear or nonlinear aggregation functions and solve them in a collaborative manner. Multiobjective evolutionary algorithm based on decomposition (MOEA/D) [6] is a representative of such approaches. Recent research indicates that decomposition-based approaches [16], [36] (e.g., MOEA/D [6]) has very good performance on MaOPs. However, the diversity of MOEA/D is maintained by a set of preset direction vectors. Very recent research has shown that performance of decomposition-based many-objective algorithms strongly depends on Pareto front shapes [37]. It is difficult for MOEA/D to maintain diversity when the shapes of PFs are irregular [38].

Some recent works focus on the hybridization of decomposition and dominance approaches [19], [20], [25], [39], [40]. For instance, Deb et al. [25], [41] proposed a reference-point-based many-objective evolutionary algorithm (NSGA-III) as an extension of NSGA-II [5]. A many-objective evolutionary algorithm based on both dominance and decomposition is also proposed to address MaOPs [19].

More recently, fifteen test problems with different shapes of PFs were proposed for CEC'2017 Competition on Evolutionary Many-Objective Optimization in [42]. This test suite aims to promote the research of MaOEA via suggesting a set of test problems with a good representation of various real-world scenarios.

To address these problems, an evolutionary many-objective optimization algorithm based on corner solution search (MaOEA-CS) was proposed. MaOEA-CS implicitly contains two phases: the exploitative search for the solutions of the most important subproblems (containing corner solutions) at the first phase, and the use of angle-based selection [1] with the explorative search for the extension of PF approximation at the second phase. Due to its high efficiency and robustness to the shapes of PFs, it has won the CEC'2017 Competition on Evolutionary Many-Objective Optimization ².

The rest of this paper is organized as follows. Section II introduces the motivations of MaOEA-CS. Section III elaborates MaOEA-CS. Section IV presents the experimental studies of MaOEA-CS on 15 MaOPs with the different number of objectives for CEC'2017 competition [42]. Section V concludes this paper.

II. DEFINITIONS AND MOTIVATIONS

A. Definitions

An MOP can be decomposed into a number of single objective optimization subproblems to be solved simultaneously in a collaborative way. A representative of such approaches is MOEA/D [6] and its variants [38], [43]–[45]. One of the most commonly used decomposition methods [2] is Weighted Sum. Let $\lambda = (\lambda_1, \dots, \lambda_m)^T$ be a direction vector for a subproblem, where $\lambda_i \geq 0$, $i \in \{1, \dots, m\}$.

1) **Weighted Sum (WS):** A subproblem is defined as

$$\begin{aligned} \text{minimize} \quad & g^{ws}(x|\lambda) = \sum_{i=1}^m \lambda_i f_i(x), \\ \text{subject to} \quad & x \in \Omega. \end{aligned} \quad (2)$$

To explain our motivations, some notations, such as the boundary direction vector, can be defined as follows.

Definition 1 (Boundary direction vector). *If a direction vector $\lambda = (\lambda_1, \dots, \lambda_m)^T$ satisfies:*

$$\exists i \in \{1, \dots, m\}, \lambda_i = 0; \quad (3)$$

Then such a vector is called a boundary direction vector.

The boundary direction vectors are the vectors with zero value for at least one objective. For instance, for a bi-objective optimization problem, the boundary direction vectors are distributed along the coordinate axis. For an m -objective optimization problem, the boundary direction vectors are distributed on any $(m-1)$ -dimensional hyperplane.

Based on the boundary direction vectors, we can further define the boundary optimal solutions as follows.

Definition 2 (Boundary optimal solution). *Given any a boundary direction vector $\lambda = (\lambda_1, \dots, \lambda_m)^T$, a boundary optimal solution $x = (x_1, \dots, x_m)^T$ can be defined as follows.*

$$x = \underset{x \in PS}{\operatorname{argmin}} g^{ws}(x|\lambda) \quad (4)$$

Obviously, the boundary optimal solutions are located on the boundaries of a PF, which contain much more information with regard to convergence than other Pareto optimal solutions. However, the number of boundary optimal solutions increase exponentially with the increase of the number of objectives. Under this circumstance, it is more practical to use some representative ones to approximate the PF boundaries. These solutions are called corner solutions, which are obtained by corner direction vectors.

Definition 3 (Corner direction vectors). *For an m -objective optimization problem, the corner direction vectors are two groups of special boundary direction vectors, V_1 and V_2 , as follows.*

$$V_1 = \{\lambda | \exists i \in \{1, 2, \dots, m\}, \lambda_i = 0 \wedge \forall j \neq i, \lambda_j = 1.\} \quad (5)$$

$$V_2 = \{\lambda | \exists i \in \{1, 2, \dots, m\}, \lambda_i = 1 \wedge \forall j \neq i, \lambda_j = 0.\} \quad (6)$$

²<http://www.cercia.ac.uk/news/cec2017maooc/>

Based on Eq. 5, only one element in a direction vector of V_1 is 0 and the other $(m-1)$ elements are 1. On the contrary, only one element in a direction vector of V_2 is 1 and the other $(m-1)$ elements are 0, based on Eq. 6.

Definition 4 (Pareto corner solution). *A set of (Pareto) corner solutions P are the boundary optimal solutions for the corner direction vector $V_1 \cup V_2$.*

For an m -objective optimization problem, the size of $V_1 \cup V_2$ is less than $2m$, thus the size of P is also less than $2m$, where m is the number of objectives. It is worth noting that multiple corner direction vectors may lead to the same corner solution.

B. motivations

Based on the concept of corner solutions, a two-phase MaOEA-CS is motivated with the following two considerations.

- 1) In the decomposition-based MOEAs, all the subproblems are treated equally important. However, the subproblems containing Pareto corner solutions are apparently more important as the corner solutions can be used to locate the ranges of PFs and help the convergence of other subproblems. Therefore, the exploitative search is favorable to be applied on them for obtaining the important corner solutions in the first phase.
- 2) After the Pareto corner solutions are approximated, the explorative search can be conducted for the extension of PF approximation in the second phase. Combined with the use of corner solutions for maintaining the convergence, the angle-based selection [1], which is robust to the shapes of PFs, is adopted for the further diversity improvement.

III. MAOEA-CS

Based on the motivations in the last section, MaOEA-CS is proposed and elaborated in this section.

A. Corner solution search

In the first phase of MaOEA-CS, two sets of the corner direction vectors are used to approximate two sets of corner solutions P_1 and P_2 . Each solution in P_1 are closest to one of the m coordinate axis as follows.

$$P_1 = \{x | x = \operatorname{argmin}_{x \in P} \operatorname{dist}^\perp(F(x), e^i), i = 1, 2, \dots, m\} \quad (7)$$

where $\operatorname{dist}^\perp(a, b)$ indicates the the perpendicular distance from a vector a to a direction vector b ; e^i denotes the direction vector along i -th axis; and P is a nondominated set.

The solutions in P_2 are closest to m hypersurfaces determined by arbitrary $(m-1)$ coordinate axis, as follows.

$$P_2 = \{x | x = \operatorname{argmin}_{x \in P} f_i(x), i = 1, 2, \dots, m\} \quad (8)$$

By combining P_1 and P_2 , the corner solution set $P_c = P_1 \cup P_2$ can be obtained. After the corner solution set P_c

($|P_c| \leq 2m$) is approximated, the nadir point z^{nad} can be further approximated as follows.

$$z^{nad} = (z_1^{nad}, z_2^{nad}, \dots, z_m^{nad})^T, \quad (9)$$

where $z_i^{nad} = \max_{x \in P_S} f_i(x) \approx \max_{x \in P_c} f_i(x)$.

The whole procedures of the corner solution search is given in Algorithm 1. P_1 is firstly obtained based on Eq. (7) and z^{nad} is approximated by P_1 based on Eq. (9). After that, P_2 is obtained based on Eq. (8). If the objective value of any solution x in P_2 is larger than that of the approximated z^{nad} , x is also added to P_c as a corner solution.

Algorithm 1 can be regarded as the combination of Pareto dominance and decomposition [6] only using $2m$ important boundary direction vectors. A very natural extension is to consider more boundary direction vectors (i.e., subproblems in MOEA/D [6]) to locate more boundaries of the PFs, which can help approximate nadir point more accurately for MaOPs with very irregular PFs. However, the appropriate balance between more subproblems for better coverage of boundary PFs and the affordable computational cost should be carefully considered, which could be an interesting research direction for the future.

Algorithm 1: Corner Solution Search (CS)

Input : P : a nondominated set;
Output: P_c : a set of corner solutions;

- 1 Obtain P_1 based on Eq (7);
- 2 $P_c = P_1$;
- 3 Estimate z^{nad} based on Eq (9);
- 4 Obtain P_2 based on Eq (8);
- 5 **for** $x \in P_2$ **do**
- 6 **for** $i = 1$ **to** m **do**
- 7 **if** $f_i(x) > z_i^{nad}$ **then**
- 8 $P_c = P_c \cup \{x\}$;
- 9 **break**;
- 10 **end**
- 11 **end**
- 12 **end**
- 13 **return** P_c ;

For instance, by using Algorithm 1, the corner solutions of four different PFs in Fig. 1 are approximated (marked in red or blue circles). At first, solutions in P_1 are selected first (marked in red circles). Then these solutions are used to approximate z^{nad} . However, in Fig. 1b, as the maximum values of solutions in P_2 (marked in blue circles) exceed the values of z^{nad} , they are also added to P_c . In fact, corner solutions are more important because they contain more information on the shapes of PFs. These solutions are very helpful to approximate the objective limitation of PFs, which can help us locate PFs.

B. The Framework of MaOEA-CS

The main procedure of MaOEA-CS is presented in Algorithm 2. At first, a population P and the corner solution set P_c are initialized. Then, the reproduction and selection steps are applied to both P and P_c iteratively until the termination criterion is fulfilled. The steps of INITIALIZATION,

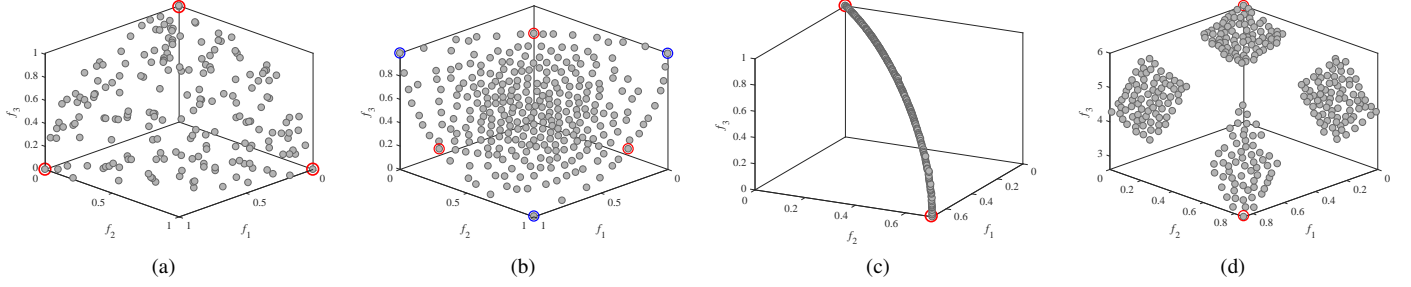


Fig. 1: Four different PF approximations and their corner solutions

REPRODUCTION, and DSA-SELECTION in Algorithm 2 are explained as follows.

Algorithm 2: Framework of MaOEA-CS (MaOEA-CS)

Input : N : Population size;
 δ : reproduction probability parameter;
 m : The number of objectives.

Output: The final population.

- 1 $[P, P_c] = \text{INITIALIZATION}(N, m)$;
 - 2 **while** *termination criterion is not fulfilled* **do**
 - 3 $Q = \text{REPRODUCTION}(P, P_c)$;
 - 4 $[P, P_c] = \text{DSA-SELECTION}(P \cup Q)$;
 - 5 **end**
 - 6 **return** P ;
-

C. Initialization

The initialization steps are given in algorithm 3. m direction vectors E along every the coordinate axes are initialized. The population P is randomly generated and then its nondominated solution set is obtained. The corner solution set P_c is also initialized by calling Algorithm 1.

Algorithm 3: Initialization (INITIALIZATION)

Input : N : population size;
 m : the number of objectives;
Output: P : The initial population;
 P_c : corner population selected from P ;

- 1 Initialize P randomly;
 /* E stores the direction vector along
 all the coordinate axes. */
 - 2 $E = (e^1, e^2, \dots, e^m)$;
 - 3 $P = \text{NONDOMINATED-SELECTION}(P)$;
 - 4 $P_c = \text{CS}(P)$;
 - 5 **return** P, P_c ;
-

D. Reproduction

Two types of reproduction, called the exploitative search and explorative search, are used in MaOEA-CS. The probability of calling exploitative or explorative search is controlled by

a parameter δ . SBX crossover [46] and polynomial mutation [47] operators are adopted as the explorative search. Meanwhile, the mutation operator in [48], [49] is adopted as the exploitative search as follows. Given a solution x , every component in x is mutated with a probability, P_m . If the i -th component of x is selected to be mutated, its offspring's i -th component x_c^i is computed by:

$$x_c^i = x^i + \text{rnd} \times (\text{ub}[i] - \text{lb}[i]),$$

$$\text{where } \text{rnd} = 0.5 \times (\text{rand} - 0.5) \times (1 - \text{rand}^\alpha), \quad (10)$$

$$\alpha = 0.7 \times \left(-1 - \frac{fe}{\text{max_fe}}\right).$$

where $\text{ub}[i]$ and $\text{lb}[i]$ are the upper and lower bound of x_i ; rand is a random number in $[0, 1]$; α is a simulated annealing variable in which fe is the current number of function evaluations and max_fe is the maximal allowable number of function evaluations.

The reproduction procedures are presented in Algorithm 4. At first, the offspring population Q is initialized to an empty set. When a random number in $[0, 1]$ is less than δ , each solution x in P_c undergoes the exploitative search for $\lfloor \frac{|P|}{|P_c|} \rfloor$ times to generate $\lfloor \frac{|P|}{|P_c|} \rfloor$ offspring where $\lfloor \bullet \rfloor$ is the floor function. All the solutions in P_c will generate N offsprings where N is the population size. When the random number in $[0, 1]$ is larger than δ , explorative search is conducted on P to generate N offspring.

As the fast convergence towards corner solutions is more important at the early stage and the extension of the corner solutions for diversity becomes more important at the late stage, δ is switched from a large number for exploitative search in the early stage to a small number $(1 - \delta)$ for explorative search at the late stage as follows.

$$\Delta_t = \max_{x \in \{1, 2, \dots, m\}} \frac{|z_i^{\text{nad}}(t) - z_i^{\text{nad}}(t - \text{len})|}{|z_i^{\text{nad}}(t - \text{len})|} \quad (11)$$

where $z_i^{\text{nad}}(t)$ indicates the i -th objective of z^{nad} approximation at the t -th iteration and len is the learning period.

If Δ_t is less than a preset small number, indicating that exploitative search has already been converged, the value of δ is switched to $(1 - \delta)$.

Algorithm 4: Reproduction (REPRODUCTION)

```

Input :  $P$ : A population;
           $P_c$ : A corner solution population;
Output:  $Q$ : Offspring population;
1  $Q = \phi$ ;
  /*  $\delta$  is a probability parameter to
  control exploitative and explorative
  search */
2 if  $rand < \delta$  then
3   for  $x \in P_c$  do
4     for  $i = 1$  to  $\lfloor \frac{|P|}{|P_c|} \rfloor$  do
5       /* Apply exploitative search on
7        $x$  according to Eq (10) */
6        $x^c = \text{EXPLOITATIVE-SEARCH}(x)$ ;
7        $Q = Q \cup \{x^c\}$ ;
8     end
9   end
10  /* Apply SBX crossover and
10  polynomial mutation on all
10  solutions in  $P$ . */
11   $Q = \text{EXPLORATIVE-SEARCH}(P)$ ;
12 end
13 return  $Q$ ;

```

E. DSA-Selection

The environmental selection of MaOEA-CS, presented in Algorithm 5, is called DSA, including dominance, space division and angle based selection, detailed as follows.

The nondominated set R_1 can be obtained from the population R by calling nondominated selection (line 1). Then, it can be used to approximate ideal point z^* as follows.

$$z^* = (z_1^*, z_2^*, \dots, z_m^*)^T, \quad (12)$$

where $z_i^* = \min_{x \in R_1} f_i(x)$.

The corner solutions are selected from R_1 by calling Algorithm 1 and z^{nad} is computed based on Eq (9). The objective space can be divided into the inside and outside space by z^* and z^{nad} , as shown in Fig. 2. Given a solution x , if there exists $i \in \{1, 2, \dots, m\}$, where $f_i(x)$ is larger than z_i^{nad} , we say x is located in the outside space. Otherwise, we say x is located in the inside space.

Based on the size of R_1 , there may three conditions, as follows.

- 1) $|R_1| > N$ (line 5 - 20): All the solutions in R_1 that are located in the inside space are added to P_{in} ; the rest solutions are added to P_{out} . When $|P_{in}| > N$, angle based selection (ABS) (Algorithm 6) is called on P_{in} to further select N solutions (line 13 - 14). When $|P_{in}| < N$, $N - |P_{in}|$ solutions closest to z^* in P_{out} are selected and added to P with P_{in} .
- 2) $|R_1| < N$ (line 21 - 23): $N - |R_1|$ solutions nearest to z^* are selected from $R \setminus R_1$ and added to P with R_1 .
- 3) $|R_1| = N$ (line 24 - 26): R_1 is assigned to P directly.

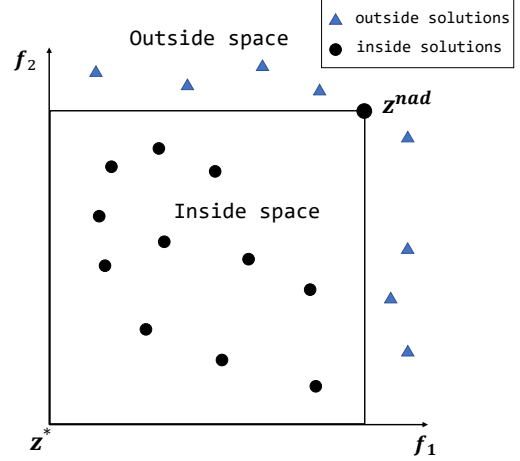


Fig. 2: An illustration of division of the inside and outside space by the nadir point approximation.

Algorithm 5: The selection of MaOEA-CS (DSA-SELECTION)

```

Input :  $R$ : The merged population ( $|R| > N$ );
Output:  $P$ : The selected solution set ( $|P| = N$ );
           $P_c$ : The corner solution set.
  /* Use fast nondominated sorting rank
  all the solutions. */
1  $R_1 = \text{NONDOMINATED-SELECTION}(R)$ ;
2 Update  $z^*$  based on Eq (12);
3  $P_c = \text{CS}(R_1)$ ;
4 Update  $z^{nad}$  based on Eq (9);
5 if  $|R_1| > N$  then
6    $P_{out} = \phi$ ;
7   foreach  $x \in R_1$  do
8     if  $\exists i \in \{1, 2, \dots, m\}, f_i(x) > z_i^{nad}$  then
9        $P_{out} = P_{out} \cup \{x\}$ ;
10    end
11  end
12   $P_{in} = R_1 \setminus P_{out}$ ;
13  if  $|P_{in}| > N$  then
14     $P = \text{ABS}(P_{in}, P_c, z^*, z^{nad})$ ;
15  else if  $|P_{in}| < N$  then
16    select  $|N - |P_{in}||$  solutions closest to  $z^*$  from
16     $P_{out}$  and add them to  $P_{in}$ ;
17     $P = P_{in}$ ;
18  else
19     $P = P_{in}$ ;
20  end
21 else if  $|R_1| < N$  then
22   Select  $|N - |R_1||$  solutions closest to  $z^*$  from  $R \setminus R_1$ 
22   and add them to  $R_1$ ;
23    $P = R_1$ ;
24 else
25    $P = R_1$ ;
26 end
27 return  $P, P_c$ ;

```

In the angle-based selection (ABS), the normalized objective vector $F'(x)$ of each solution x can be obtained as follows.

$$F'(x) = (f'_1(x), f'_2(x), \dots, f'_m(x))^T, \quad (13)$$

where $f'_i(x) = \frac{f_i(x) - z_i^*}{z_i^{nad} - z_i^*}$.

The angle between two solutions, x and y , can be calculated by:

$$angle(x, y) = \arccos\left(\frac{F'(x)^T \cdot F'(y)}{\|F'(x)\| \|F'(y)\|}\right) \quad (14)$$

The procedures of ABS are presented in Algorithm 6. The corner solutions are firstly added to P and deleted from Q . For i -th solution in Q , θ_i is used to record the minimal angle from it to its nearest solution in P . The solution with maximal θ is added to P and deleted from Q one by one until the population size of P reaches N . If the angle between each solution in Q with newly added solution x is larger than its previous θ , θ is updated by the angle value.

It is worth noting that ABS works similarly to the weight setting method in [50], except that ABS uses angles to select solutions while distances are used in [50] to select weight vectors (direction vectors).

Algorithm 6: The angle based selection (ABS)

Input : Q : A population whose size is larger than N ;
 P_c : The corner solution population;
 z^* : The ideal point;
 z^{nad} : The nadir point.

Output: P : A population whose size is equal to N ;

- 1 $P = \phi$;
- 2 $P = P \cup P_c$;
- 3 $Q = Q \setminus P_c$;
- 4 $\theta = (\theta_1, \theta_2, \dots, \theta_{|Q|})$;
- 5 **foreach** $x^i \in Q$ **do**
- 6 $\theta_i = \min_{x^j \in P} \{angle(x^i, x^j)\}$;
- 7 **end**
- 8 **while** $|P| < N$ **do**
- 9 $k = \operatorname{argmax}_{k \in \{1, 2, \dots, |Q|\}} \{\theta_k\}$;
- 10 $Q = Q \setminus \{x^k\}$;
- 11 $\theta = \theta \setminus \{\theta^k\}$;
- 12 $P = P \cup \{x^k\}$;
- 13 **foreach** $\theta_j \in \theta$ **do**
- 14 $\theta_j = \max\{\theta_j, angle(x^k, x^j)\}$;
- 15 **end**
- 16 **end**
- 17 **return** P ;

IV. EXPERIMENTAL RESULTS

In this section, MaOEA-CS is compared with six state-of-the-art algorithms (BCE-MOEA/D [51], KnEA [23], RVEA [24], NSGA-III [25], GSRA [52] and RSEA [53]), in the CEC'2017 Competition on Evolutionary Many-Objective Optimization.

TABLE I: The characteristics of the MaF test suite [42].

Problem	Characteristics
MaF1	Linear, No single optimal solution in any subset of objectives
MaF2	Concave, No single optimal solution in any subset of objectives
MaF3	Convex, Multimodal
MaF4	Concave, Multimodal, Badly-scaled, No single optimal solution in any subset of objectives
MaF5	Convex, Biased, Badly-scaled
MaF6	Concave, Degenerate
MaF7	Mixed, Disconnected, Multimodal
MaF8	Linear, Degenerate
MaF9	Linear, Degenerate
MaF10	Mixed, Biased
MaF11	Convex, Disconnected, Nonseparable
MaF12	Concave, Nonseparable, Biased Deceptive
MaF13	Concave, Unimodal, Nonseparable, Degenerate, Complex Pareto set
MaF14	Linear, Partially separable, Large scale
MaF15	Convex, Partially separable, Large scale

A. Benchmark problems

Fifteen benchmark functions were proposed in [42] for CEC2017 competition on evolutionary many-objective optimization. Different from other test suites, the problems in this test suite contain more irregular PFs, aiming to represent various real-world scenarios. The characteristics of all the test instances are summarized in Table I. For each test instance, the number of objectives is set to $m \in \{5, 10, 15\}$ respectively and the number of variables is set as suggested in [42].

B. Parameter settings

The population size, the termination criterion and the running time are set as suggested in [42]. In the reproduction step, δ is set to 0.9; the crossover probability p_c is set to 1; the distribution index η_c is set to 20 for SBX; the mutation probability p_m is set to $1/D$, where D is the number of decision variables; the distribution index η_m for polynomial mutation is set to 20; Δ_t is set to $0.001 \times m$ where m is the number of objectives and the learning period len is set to 50. The algorithm is programmed in MATLAB and embedded in the open-source MATLAB software platform platEMO [54], suggested by [42]. The parameters in other algorithms are set the same as the original papers.

Each instance was run 31 times. In each run, the maximal allowed number of function evaluations is set to $\max\{100000; 10000 \times D\}$ where D is the number of variables. The population sizes of all the compared algorithms are set to $m \times 25$ where m is the number of objectives.

C. Performance Metrics

IGD [55]–[57] and HV [34] are two widely used performance metrics. Both of them can simultaneously measure the convergence and diversity of the obtained solution set, as follows.

- Inverted Generational Distance (IGD): Let P^* be a set of points uniformly sampled over the true PF, and S be the set of solutions obtained by an EMO algorithm. The IGD value of S is computed as:

$$IGD(S, P^*) = \frac{\sum_{x \in P^*} dist(x, S)}{|P^*|} \quad (15)$$

where $dist(x, S)$ is the Euclidean distance between a point $x \in P^*$ and its nearest neighbor in S , and $|P^*|$ is the cardinality of P^* . The lower is the IGD value, the better is the quality of S for approximating the whole PF.

- Hypervolume (HV): Let $r^* = (r_1^*, r_2^*, \dots, r_m^*)^T$ be a reference point in the objective space that is dominated by all the PF approximation S . HV metric measures the size of the objective space dominated by the solutions in S and bounded by r^* .

$$HV(S) = VOL\left(\bigcup_{x \in S} [f_1(x), r_1^*] \times \dots [f_m(x), r_m^*]\right) \quad (16)$$

where $VOL(\bullet)$ indicates the Lebesgue measure. Hypervolume can measure the approximation in terms of both diversity and convergence. The larger the HV value, the better the quality of PF approximation S is.

In this paper, Monte Carlo sampling method [58] is used to compute HV values. It is worth noting that both IGD and HV values of the nondominated set obtained by all the compared algorithms are computed by platEMO [54].

D. Empirical Results And Discussion

Table. II shows the performance of seven compared algorithms in terms of mean IGD over 31 runs while Table. III shows the performance of seven compared algorithms in terms of mean HV over 31 runs. In addition, the overall rankings of seven compared algorithms on all the test problems are presented in Table. IV. It can be observed clearly that the mean rank of all 45 problems for MaOEA-CS in terms of IGD and HV are 2.69 and 2.98, respectively, which won the first ranks among all the seven compared algorithms. This indicates that MaOEA-CS has the best overall performance for MaOPs with different characteristics.

MaF1 has an inverted linear PF. MaOEA-CS performs best on 5-, 10- and 15-objective MaF1, in terms of IGD, among all the compared algorithms. However, MaOEA-CS performs worse than other compared algorithms, in terms of HV. Especially on 15-objective MaF1, the HV value of the nondominated set obtained by MaOEA-CS is 0. It can be explained as follows. As Monte Carlo sampling method is adopted to compute HV and the true HV for MaF1 (inverted PF) is very small [37], [41], the limited sampling in the hypercube can hardly fall into the region determined by the nondominated set and the reference point.

To further verify the performance of all the compared algorithms in MaF1, the parallel coordinate plots [59] of the nondominated sets obtained by various algorithms on 15-objective MaF1 in the run with the median IGD values are presented in Fig. 3. It can be observed clearly that MaOEA-CS finds all the boundary solutions and the uniformity of approximation is better than all the other compared algorithms. The

convergence of MaOEA-CS is also better than that of other compared algorithms as all the objective values of the solutions obtained by MaOEA-CS are less than 1.0. KnEA, RSEA and GSRA are worse in terms of diversity or convergence. NSGA-III performs worse in terms of diversity and BCE-MOEA/D performs worse in terms of convergence. RVEA is not able to obtain the sufficient number of nondominated solutions.

MaF2 is used to assess whether the MaOEA is able to perform concurrent convergence on different objectives. All the objectives should be optimized simultaneously to well-approximate the true PF. It can be observed from the tables that MaOEA-CS has the best performance in terms of IGD on 5-objective MaF2, while KnEA has the best performance on 10- and 15-objective MaF2. As for HV values, GSRA and RSEA perform better than other compared algorithms.

MaF3 is a multimodel problem with the convex PF. This problem is mainly to test whether the MaOEA can deal with convex PFs. It can be observed from the tables that MaOEA-CS has the best performance on MaF3 (5, 10, 15-objectives), in terms of HV, while GSRA has the best performance in terms of IGD.

MaF4 is also a multimodel problem with THE convex PF, but it is more difficult than MaF3 as it is not well-scaled. It can be observed from the tables that MaOEA-CS performs best on all MaF4 problems, in terms of IGD while it only has the best performance on 5-objective MaF4 in terms of HV. NSGA-III and RSEA have the best performance, in terms of HV, on 10- and 15-objective MaF3, respectively.

The PS of MaF5 has a highly biased distribution, where the majority of Pareto optimal solutions are crowded in a small subregion. In addition, MaF5 is also a badly-scaled problem with objective values ranging from 1 to 1024. It can be observed from the tables that MaOEA-CS has the best performance in terms of IGD, while NSGA-III have the best performance, in terms of HV, on 10-objective MaF5 and KnEA has the best performance in terms of HV, on 15-objective MaF5.

MaF6 is a degenerated problem whose PF is a 2-dimensional manifold regardless of the number of objectives. It can be observed from the tables that MaOEA-CS has the best performance in terms of IGD and HV on all the MaF6 with different number of objectives, except for 10-objective MaF6, where BCE-MOEA/D has the best performance in terms of IGD.

MaF7 has a disconnected PF where the number of disconnected segments is $2^m - 1$ (m is the number of objectives). MaF7 can be used to test whether an MaOEA can handle MaOPs with the disconnected PFs. It can be observed from the tables that GSEA and KnEA performs better in terms of IGD and RSEA performs better in terms of HV. MaOEA-CS performs well in terms of both IGD and HV, although it does not have the best performance.

Both MaF8 and MaF9 have two-dimensional decision space. MaF8 calculates the Euclidean distance from a given point x to a set of M target points of a given polygon while MaF9 calculates the Euclidean distance from x to a set of M target straight lines, each of which passes through an edge of the given regular polygon with M vertexes. It can be observed

TABLE II: The performance of seven compared algorithms, in terms of IGD values on MaF1-15.

Problem	m	BCE-MOEA/D	GSRA	KnEA	RSEA	RVEA	NSGA-III	MaOEA-CS
MaF1	5	1.429E-01 (9.3E-04) ⁻	1.336E-01 (1.4E-03) ⁻	1.246E-01 (2.1E-03) ⁻	1.479E-01 (2.9E-03) ⁻	3.249E-01 (1.2E-01) ⁻	2.073E-01 (1.1E-02) ⁻	1.226E-01 (7.5E-04)
	10	2.555E-01 (1.3E-02) ⁻	2.512E-01 (4.7E-03) ⁻	2.307E-01 (3.3E-03) ⁻	2.425E-01 (4.0E-03) ⁻	6.395E-01 (5.9E-02) ⁻	2.820E-01 (1.6E-02) ⁻	2.273E-01 (1.3E-03)
	15	3.869E-01 (9.6E-03) ⁻	2.925E-01 (6.2E-03) ⁻	2.760E-01 (4.7E-03) ⁻	2.888E-01 (6.7E-03) ⁻	7.000E-01 (7.1E-02) ⁻	3.159E-01 (6.9E-03) ⁻	2.536E-01 (1.2E-03)
MaF2	5	1.073E-01 (1.6E-03) ⁻	1.145E-01 (2.8E-03) ⁻	1.309E-01 (3.6E-03) ⁻	1.255E-01 (4.1E-03) ⁻	1.279E-01 (1.2E-03) ⁻	1.309E-01 (2.7E-03) ⁻	1.006E-01 (1.3E-03)
	10	1.758E-01 (4.8E-03) ⁺	1.630E-01 (3.5E-03) ⁺	1.569E-01 (6.6E-03) ⁺	3.181E-01 (1.5E-02) ⁻	3.670E-01 (2.0E-01) ⁻	2.180E-01 (3.3E-02) ⁺	2.424E-01 (2.2E-02)
	15	1.976E-01 (1.1E-02) ⁺	1.899E-01 (6.0E-03) ⁺	1.812E-01 (4.6E-03) ⁺	2.823E-01 (1.4E-02) ⁺	6.401E-01 (1.9E-01) ⁻	2.100E-01 (8.0E-03) ⁺	4.250E-01 (2.0E-02)
MaF3	5	1.347E-01 (1.4E-02) ⁻	7.647E-02 (4.2E-03) ⁺	1.597E-01 (7.2E-02) ⁻	9.274E-02 (3.4E-02) ⁺	9.355E-02 (4.3E-02) ⁻	9.743E-02 (1.1E-03) ⁺	1.015E-01 (2.4E-03)
	10	4.546E-01 (2.8E-01) ⁻	8.343E-02 (4.5E-03) ⁺	4.935E+07 (2.6E+08) ⁻	2.583E+02 (5.5E+02) ⁻	1.324E-01 (7.2E-02) ⁻	3.337E+03 (1.1E+04) ⁻	1.049E-01 (3.1E-03)
	15	3.984E-01 (3.7E-01) ⁻	8.759E-02 (2.4E-03) ⁺	1.914E+09 (5.2E+09) ⁻	7.988E+02 (1.4E+03) ⁻	9.320E-02 (3.9E-03) ⁺	1.853E+03 (6.0E+03) ⁻	1.013E-01 (3.2E-03)
MaF4	5	3.429E+00 (4.9E-01) ⁻	2.827E+00 (2.1E-01) ⁻	2.803E+00 (2.8E-01) ⁻	2.936E+00 (1.9E-01) ⁻	4.696E+00 (8.7E-01) ⁻	3.524E+00 (2.6E-01) ⁻	2.186E+00 (5.3E-02)
	10	7.807E+01 (9.7E+00) ⁻	1.408E+02 (1.5E+01) ⁻	7.874E+01 (8.0E+00) ⁻	1.012E+02 (6.2E+00) ⁻	2.005E+02 (5.1E+01) ⁻	9.475E+01 (8.3E+00) ⁻	5.290E+01 (2.4E+00)
	15	3.545E+03 (6.9E+02) ⁻	4.366E+03 (6.9E+02) ⁻	2.854E+03 (4.6E+03) ⁻	2.838E+03 (2.9E+02) ⁻	7.325E+03 (1.5E+03) ⁻	3.877E+03 (3.3E+02) ⁻	1.543E+03 (1.7E+02)
MaF5	5	2.275E+00 (4.5E-02) ⁻	2.346E+00 (5.5E-02) ⁻	2.451E+00 (5.9E-02) ⁻	2.514E+00 (1.9E-01) ⁻	2.385E+00 (4.5E-01) ⁻	2.540E+00 (9.9E-01) ⁻	2.074E+00 (3.3E-02)
	10	9.466E+01 (4.8E+00) ⁻	5.878E+01 (5.9E+00) ⁻	7.901E+01 (7.4E+00) ⁻	7.975E+01 (1.5E+01) ⁻	1.051E+02 (1.1E+01) ⁻	8.988E+01 (8.9E+00) ⁻	4.727E+01 (1.7E+00)
	15	2.828E+03 (2.9E-02) ⁻	1.261E+03 (2.8E-02) ⁻	1.725E+03 (1.7E-02) ⁻	2.097E+03 (4.9E-02) ⁻	3.604E+03 (7.0E-02) ⁻	2.533E+03 (8.3E+01) ⁻	1.101E+03 (7.7E+01)
MaF6	5	4.181E-03 (4.2E-05) ⁻	6.088E-03 (3.8E-04) ⁻	6.068E-03 (6.5E-04) ⁻	2.943E-01 (7.6E-02) ⁻	8.990E-02 (1.8E-02) ⁻	5.152E-02 (3.8E-02) ⁻	4.026E-03 (1.4E-04)
	10	2.102E-03 (4.1E-05) ⁺	2.473E+00 (8.7E-01) ⁻	8.877E+00 (7.0E+00) ⁻	2.548E-01 (6.7E-02) ⁻	1.275E-01 (2.5E-02) ⁻	3.527E+00 (1.6E+01) ⁻	2.599E-03 (2.2E-05)
	15	2.125E-03 (3.7E-05) ⁻	2.873E+00 (8.1E-01) ⁻	2.104E+01 (1.2E+01) ⁻	5.497E-01 (2.6E-01) ⁻	3.158E-01 (2.5E-01) ⁻	6.869E+00 (1.0E+01) ⁻	1.913E-03 (1.1E-04)
MaF7	5	3.182E-01 (1.3E-02) ⁺	2.995E-01 (3.2E-02) ⁺	2.991E-01 (1.1E-02) ⁺	4.512E-01 (8.5E-02) ⁻	4.483E-01 (7.8E-04) ⁻	3.366E-01 (1.7E-02) ⁻	3.277E-01 (8.7E-03)
	10	8.688E-01 (2.1E-02) ⁺	8.445E-01 (6.9E-03) ⁺	8.662E-01 (7.4E-03) ⁺	6.626E-01 (3.5E-01) ⁻	2.819E+00 (2.7E-01) ⁻	1.216E+00 (1.1E-01) ⁻	8.983E-01 (1.6E-02)
	15	1.663E+00 (1.4E-01) ⁺	1.389E+00 (6.0E-03) ⁺	2.345E+00 (2.5E-01) ⁻	6.576E+00 (9.9E-01) ⁻	4.031E+00 (7.5E-01) ⁻	3.266E+00 (4.5E-01) ⁻	1.781E+00 (9.3E-02)
MaF8	5	1.088E-01 (1.3E-03) ⁻	9.537E-02 (1.6E-03) ⁺	2.666E-01 (7.3E-02) ⁻	1.379E-01 (2.4E-02) ⁻	4.633E-01 (5.7E-02) ⁻	2.594E-01 (3.4E-02) ⁻	1.026E-01 (1.7E-03)
	10	1.098E-01 (7.6E-04) ⁺	1.612E-01 (6.7E-02) ⁻	1.592E-01 (2.1E-02) ⁻	1.709E-01 (1.3E-02) ⁻	8.082E-01 (9.4E-02) ⁻	3.816E-01 (6.4E-02) ⁻	1.154E-01 (2.9E-03)
	15	1.329E-01 (9.7E-04) ⁻	4.196E+00 (4.4E+00) ⁻	1.534E-01 (3.4E-02) ⁻	1.796E-01 (1.7E-02) ⁻	1.320E+00 (2.3E-01) ⁻	3.470E-01 (6.3E-02) ⁻	1.227E-01 (4.3E-03)
MaF9	5	1.912E-01 (3.4E-02) ⁻	9.083E-02 (7.4E-04) ⁺	7.392E-01 (3.3E-01) ⁻	4.757E-01 (1.9E-01) ⁻	3.784E-01 (7.2E-02) ⁻	3.059E-01 (6.3E-02) ⁻	1.436E-01 (3.7E-02)
	10	1.444E+00 (3.2E-03) ⁻	1.038E-01 (8.9E-04) ⁺	6.004E+01 (4.9E+01) ⁻	1.423E-01 (1.8E-02) ⁻	8.159E-01 (2.0E-01) ⁻	5.955E-01 (1.8E-01) ⁻	1.214E-01 (1.6E-02)
	15	1.584E+00 (1.9E-01) ⁻	1.071E-01 (8.2E-03) ⁺	3.410E-01 (2.7E-01) ⁻	2.912E-01 (2.0E-01) ⁻	1.689E+00 (1.9E+00) ⁻	1.115E+00 (2.8E+00) ⁻	1.477E-01 (4.4E-02)
MaF10	5	5.167E-01 (7.7E-03) ⁺	8.642E-01 (1.0E-01) ⁻	5.185E-01 (2.3E-02) ⁺	5.225E-01 (3.2E-02) ⁺	4.520E-01 (3.9E-02) ⁺	4.580E-01 (1.3E-02) ⁺	5.383E-01 (4.9E-02)
	10	1.309E+00 (4.5E-02) ⁺	1.603E+00 (2.2E-01) ⁺	1.191E+00 (1.2E-01) ⁺	1.282E+00 (1.6E-01) ⁺	1.283E+00 (5.9E-02) ⁺	1.094E+00 (5.5E-02) ⁺	1.794E+00 (1.6E-01)
	15	1.678E+00 (5.9E-02) ⁺	2.073E+00 (1.8E-01) ⁺	1.623E+00 (1.1E-01) ⁺	1.739E+00 (1.4E-01) ⁺	1.844E+00 (2.0E-01) ⁺	1.615E+00 (3.2E-01) ⁺	2.791E+00 (4.2E-01)
MaF11	5	6.049E-01 (3.2E-02) ⁺	2.155E+00 (4.2E-01) ⁻	6.690E-01 (1.2E-01) ⁺	6.729E-01 (6.7E-02) ⁺	1.556E+00 (5.5E-01) ⁻	8.185E-01 (2.8E-02) ⁺	8.228E-01 (4.6E-02)
	10	1.614E+00 (3.0E-01) ⁺	9.216E+00 (1.5E+00) ⁻	2.416E+00 (4.2E-01) ⁺	2.354E+00 (2.5E-01) ⁺	7.340E+00 (2.1E+00) ⁻	5.632E+00 (2.0E+00) ⁻	2.576E+00 (1.7E-01)
	15	3.378E-01 (2.6E-01) ⁻	1.837E+01 (2.2E+00) ⁻	5.299E+00 (1.1E+00) ⁻	1.689E+00 (1.8E+00) ⁻	1.941E+01 (3.6E+00) ⁻	1.293E+01 (1.6E+00) ⁻	1.568E-01 (8.3E-02)
MaF12	5	1.181E+00 (3.5E-02) ⁻	1.180E+00 (1.3E-02) ⁻	1.176E+00 (1.6E-02) ⁻	1.274E+00 (4.9E-02) ⁻	1.122E+00 (2.6E-03) ⁻	1.119E+00 (6.2E-03) ⁻	1.106E+00 (2.4E-02)
	10	4.492E+00 (7.9E-02) ⁻	4.344E+00 (1.0E-01) ⁻	4.553E+00 (4.9E-02) ⁻	4.706E+00 (9.0E-02) ⁻	4.491E+00 (6.2E-02) ⁻	4.574E+00 (9.8E-02) ⁻	4.045E+00 (3.4E-02)
	15	6.950E+00 (1.9E-01) ⁻	7.522E+00 (1.6E-01) ⁻	6.528E+00 (1.1E-01) ⁻	8.389E+00 (1.9E-01) ⁻	7.069E+00 (2.1E-01) ⁻	8.139E+00 (2.6E-01) ⁻	6.501E+00 (1.2E-01)
MaF13	5	1.549E-01 (1.0E-02) ⁺	1.076E-01 (1.2E-02) ⁺	2.219E-01 (1.8E-02) ⁺	2.281E-01 (2.3E-02) ⁺	6.352E-01 (1.3E-01) ⁻	2.442E-01 (1.6E-02) ⁺	2.511E-01 (7.5E-02)
	10	1.316E-01 (4.7E-03) ⁺	9.634E-02 (1.2E-02) ⁺	1.878E-01 (2.5E-02) ⁺	2.798E-01 (4.2E-02) ⁺	9.889E-01 (2.8E-01) ⁺	2.291E-01 (2.8E-02) ⁺	1.315E+00 (1.7E-01)
	15	1.449E-01 (7.9E-03) ⁺	1.030E-01 (1.5E-02) ⁺	1.818E-01 (2.5E-02) ⁺	3.265E-01 (7.7E-02) ⁺	1.192E+00 (4.6E-01) ⁺	2.583E-01 (3.4E-02) ⁺	1.672E+00 (2.5E-01)
MaF14	5	5.257E-01 (5.0E-02) ⁻	4.951E-01 (2.9E-02) ⁻	5.695E-01 (8.3E-02) ⁻	6.712E-01 (2.0E-01) ⁻	7.144E-01 (2.0E-01) ⁻	6.937E-01 (1.8E-01) ⁻	4.475E-01 (7.9E-02)
	10	7.787E-01 (7.2E-02) ⁻	1.486E+00 (7.2E-01) ⁻	2.517E+01 (3.9E+01) ⁻	1.587E+00 (5.6E-01) ⁻	6.664E-01 (5.8E-02) ⁺	1.768E+00 (6.7E-01) ⁻	4.045E+00 (3.4E-02)
	15	1.089E+00 (2.5E-01) ⁻	1.606E+00 (2.9E-01) ⁻	1.208E+01 (4.4E+00) ⁻	9.096E-01 (2.5E-01) ⁻	8.518E-01 (1.7E-01) ⁺	1.331E+00 (2.1E-01) ⁻	8.773E-01 (1.3E-01)
MaF15	5	1.157E+00 (1.7E-01) ⁻	4.094E-01 (2.4E-02) ⁺	4.020E+00 (1.7E+00) ⁻	1.100E+00 (5.3E-02) ⁻	6.004E-01 (4.4E-02) ⁻	1.291E+00 (9.2E-02) ⁻	4.700E-01 (6.8E-02)
	10	2.338E+00 (4.8E-01) ⁻	6.175E-01 (1.6E-01) ⁺	5.772E+00 (5.1E+00) ⁻	1.347E+00 (4.6E-02) ⁻	9.843E-01 (3.4E-02) ⁻	1.436E+00 (1.9E-01) ⁻	9.272E-01 (6.4E-02)
	15	3.454E+00 (7.2E-01) ⁻	1.078E+00 (3.6E-02) ⁺	9.367E+01 (5.6E+01) ⁻	1.445E+00 (5.2E-02) ⁻	1.167E+00 (2.8E-02) ⁻	3.656E+00 (2.1E+00) ⁻	1.106E+00 (4.0E-02)

Wilcoxon's rank sum test at a 0.05 significance level is performed in terms of IGD values. "+", "-" or "≈" indicate that the results obtained by corresponding algorithms is significantly better, worse or similar to that of MaOEA-CS on this test instance, respectively.

from Table. IV that, although MaOEA-CS does not obtain the best performance, it always ranks the first or second among all the seven compared algorithms. This indicates that MaOEA-CS has more stable performance on MaF8-9.

MaF10 has a scaled PF containing both convex and concave segments, which is used to test whether the algorithm can handle PFs of complicated and mixed geometries. It can be observed from the tables that NSGA-III and RVEA perform better in terms of IGD; while NSGA-III performs better in terms of HV.

MaF11 is used to assess whether an MaOEA is capable of handle an MaOP with the scaled and disconnected PFs. It can be observed from the tables that BCE-MOEA/D and MaOEA-CS perform better in terms of IGD; while NSGA-III and RSEA performs better in terms of HV.

As for MaF12, its decision variables are nonseparably reduced, and its fitness landscape is highly multimodal. It can be observed from the tables that MaOEA-CS has the

best performance in terms of IGD; while KnEA has the best performance in terms of HV.

MaF13 has a simple concave PF that is always a unit sphere regardless of the number of objectives. However, its decision variables are nonlinearly linked with the first and second decision variables, thus leading to difficulty in convergence. This problem is used to test whether the algorithm can handle an MaOP with the complicated PS. GSRA has the best performance in terms of both IGD and HV.

MaF14 and MaF15 are mainly used to assess whether an MaOEA can handle complicated fitness landscape with mixed variable separability, especially in large-scale cases. MaOEA-CS has very good overall performance as it can be observed from Table. IV that MaOEA-CS ranks either first or second among all the seven compared algorithms in terms of HV or IGD.

TABLE III: The performance of seven compared algorithms, in terms of HV values, on MaF1-15.

Problem	m	BCE-MOEA/D	GSRA	KnEA	RSEA	RVEA	NSGA-III	MaOEA-CS
MaF1	5	9.052E-03 (9.6E-05) ⁻	8.700E-03 (1.9E-04) ⁻	1.058E-02 (1.8E-04) ⁻	9.371E-03 (1.3E-04) ⁻	2.269E-03 (8.4E-04) ⁻	4.720E-03 (5.4E-04) ⁻	1.104E-02 (1.2E-04)
	10	3.870E-07 (1.4E-07) ⁺	2.426E-07 (3.9E-07) ⁻	3.793E-07 (1.3E-07) ⁺	5.812E-07 (9.8E-08) ⁺	5.963E-09 (2.7E-09) ⁻	3.253E-07 (6.2E-08) ⁻	3.226E-07 (5.4E-07)
	15	8.063E-13 (9.3E-14) ⁺	0.000E+00 (0.0E+00) [≈]	0.000E+00 (0.0E+00) [≈]	1.229E-11 (1.5E-11) ⁺	2.913E-14 (2.4E-14) ⁺	3.435E-12 (9.0E-13) ⁺	0.000E+00 (0.0E+00)
MaF2	5	1.795E-01 (2.1E-03) ⁻	1.885E-01 (1.7E-03) ⁺	1.869E-01 (1.9E-03) [≈]	1.816E-01 (2.2E-03) ⁻	1.509E-01 (2.3E-03) ⁻	1.516E-01 (4.1E-03) ⁻	1.845E-01 (2.4E-03)
	10	1.825E-01 (5.1E-03) ⁻	2.197E-01 (3.5E-03) ⁺	1.682E-01 (1.2E-02) ⁻	2.382E-01 (2.1E-03) ⁺	1.577E-01 (5.1E-02) ⁻	2.093E-01 (9.7E-03) ⁻	2.127E-01 (5.8E-03)
	15	1.291E-01 (8.5E-03) ⁻	2.133E-01 (3.4E-03) ⁻	1.063E-01 (1.2E-02) ⁻	2.333E-01 (3.1E-03) ⁺	6.223E-02 (2.0E-02) ⁻	1.409E-01 (9.6E-03) ⁻	2.289E-01 (6.0E-03)
MaF3	5	9.844E-01 (9.6E-03) ⁻	9.899E-01 (2.4E-03) ⁻	9.534E-01 (6.7E-02) ⁻	9.921E-01 (2.7E-02) ⁻	9.906E-01 (2.2E-02) ⁻	9.987E-01 (9.8E-05) [≈]	9.988E-01 (8.1E-05)
	10	5.583E-01 (2.5E-01) ⁻	9.982E-01 (6.5E-04) ⁻	0.000E+00 (0.0E+00) ⁻	1.099E-01 (2.7E-01) ⁻	9.817E-01 (5.8E-02) ⁻	5.230E-02 (2.0E-01) ⁻	1.000E+00 (9.2E-06)
	15	6.675E-01 (3.5E-01) ⁻	9.997E-01 (2.2E-04) ⁻	0.000E+00 (0.0E+00) ⁻	0.000E+00 (0.0E+00) ⁻	9.995E-01 (3.4E-04) ⁻	1.233E-01 (3.2E-01) ⁻	1.000E+00 (4.4E-07)
MaF4	5	2.501E-02 (4.9E-03) ⁻	6.788E-02 (6.0E-03) ⁻	1.061E-01 (6.0E-03) [≈]	1.031E-01 (2.0E-03) ⁻	1.412E-02 (8.3E-03) ⁻	5.769E-02 (8.2E-03) ⁻	1.061E-01 (1.9E-03)
	10	3.983E-06 (5.0E-06) ⁻	1.852E-06 (6.2E-07) ⁻	9.675E-05 (3.4E-05) ⁺	3.953E-04 (1.5E-05) ⁺	1.518E-07 (2.7E-07) ⁻	2.067E-04 (1.6E-05) ⁺	5.210E-05 (1.3E-05)
	15	1.357E-09 (3.2E-09) ⁺	8.956E-12 (7.9E-12) ⁺	1.495E-09 (8.3E-09) ⁺	4.775E-07 (2.6E-08) ⁺	4.759E-13 (4.8E-13) ⁺	2.482E-07 (2.4E-08) ⁺	0.000E+00 (0.0E+00)
MaF5	5	7.728E-01 (5.1E-03) ⁻	7.114E-01 (2.5E-02) ⁻	7.752E-01 (4.3E-03) ⁻	7.599E-01 (9.3E-03) ⁻	7.650E-01 (3.4E-02) ⁻	7.632E-01 (4.4E-02) ⁻	7.821E-01 (2.5E-03)
	10	8.738E-01 (3.0E-02) ⁻	8.020E-01 (3.0E-02) ⁻	9.538E-01 (5.4E-03) [≈]	9.220E-01 (8.8E-03) ⁻	9.536E-01 (6.4E-03) [≈]	9.664E-01 (7.2E-03) ⁺	9.538E-01 (1.9E-03)
	15	8.643E-01 (5.2E-02) ⁻	9.337E-01 (1.8E-02) ⁻	9.946E-01 (4.1E-04) ⁺	9.686E-01 (4.6E-03) ⁻	9.440E-01 (7.9E-03) ⁻	9.905E-01 (3.2E-03) ⁺	9.855E-01 (2.5E-03)
MaF6	5	1.296E-01 (4.3E-04) [≈]	1.278E-01 (4.5E-04) ⁻	1.284E-01 (3.7E-04) [≈]	1.243E-01 (3.8E-03) ⁻	1.148E-01 (3.2E-03) ⁻	1.226E-01 (5.0E-03) ⁻	1.298E-01 (3.9E-04)
	10	1.010E-01 (3.7E-04) [≈]	0.000E+00 (0.0E+00) ⁻	0.000E+00 (0.0E+00) ⁻	7.996E-02 (2.7E-02) ⁻	8.571E-02 (2.0E-02) ⁻	4.302E-02 (3.1E-02) ⁻	1.000E+00 (9.2E-06)
	15	9.541E-02 (2.7E-04) [≈]	0.000E+00 (0.0E+00) ⁻	0.000E+00 (0.0E+00) ⁻	1.018E-02 (2.3E-02) ⁻	9.161E-02 (7.2E-04) ⁻	1.571E-02 (2.7E-02) ⁻	9.557E-02 (2.7E-04)
MaF7	5	2.012E-01 (8.3E-03) [≈]	2.456E-01 (2.7E-03) ⁻	2.546E-01 (5.3E-03) ⁺	2.518E-01 (8.2E-03) [≈]	2.152E-01 (7.0E-04) ⁻	2.373E-01 (5.6E-03) ⁻	2.501E-01 (2.6E-03)
	10	1.458E-01 (4.0E-03) ⁻	9.392E-02 (2.7E-02) ⁻	8.096E-02 (3.0E-02) ⁻	1.908E-01 (7.0E-03) ⁺	1.492E-01 (1.7E-02) ⁻	1.386E-01 (9.7E-03) ⁻	1.695E-01 (7.2E-03)
	15	1.142E-02 (1.4E-02) ⁻	7.456E-03 (4.0E-03) ⁻	2.212E-03 (1.1E-02) ⁻	1.614E-01 (6.3E-03) ⁺	6.956E-02 (5.9E-02) ⁻	3.199E-02 (8.1E-03) ⁻	1.341E-01 (3.1E-03)
MaF8	5	1.168E-01 (5.7E-04) ⁻	1.224E-01 (4.2E-04) [≈]	1.010E-01 (1.1E-02) ⁻	1.190E-01 (1.6E-03) ⁻	7.164E-02 (7.5E-03) ⁻	8.659E-02 (5.9E-03) ⁻	1.215E-01 (4.4E-04)
	10	1.036E-02 (1.0E-04) ⁻	1.062E-02 (3.1E-04) ⁻	1.019E-02 (2.4E-04) ⁻	1.106E-02 (7.1E-05) [≈]	4.665E-03 (8.1E-04) ⁻	8.885E-03 (3.2E-04) ⁻	1.097E-02 (1.1E-04)
	15	5.837E-04 (1.7E-05) ⁻	2.429E-04 (2.7E-04) ⁻	6.027E-04 (5.4E-05) ⁻	6.814E-04 (1.6E-05) ⁺	1.164E-04 (3.8E-05) ⁻	5.020E-04 (2.9E-05) ⁻	6.575E-04 (2.5E-05)
MaF9	5	2.749E-01 (1.4E-02) ⁻	3.148E-01 (7.9E-04) ⁺	1.369E-01 (5.0E-02) ⁻	1.886E-01 (5.1E-02) ⁻	1.915E-01 (1.8E-02) ⁻	2.257E-01 (2.1E-02) ⁻	2.920E-01 (1.3E-02)
	10	2.292E-03 (1.2E-05) ⁻	1.854E-02 (1.5E-04) [≈]	3.201E-05 (1.8E-04) ⁻	1.680E-02 (8.4E-04) ⁻	4.694E-03 (8.3E-04) ⁻	8.166E-03 (1.9E-03) ⁻	1.851E-02 (2.3E-04)
	15	1.739E-04 (3.7E-05) ⁻	1.387E-03 (4.0E-05) ⁺	1.087E-03 (2.7E-04) ⁻	1.081E-03 (3.3E-04) ⁻	2.075E-04 (8.7E-05) ⁻	7.837E-04 (2.2E-04) ⁻	1.339E-03 (1.1E-04)
MaF10	5	9.976E-01 (1.2E-04) ⁺	6.898E-01 (4.7E-02) ⁻	9.896E-01 (1.8E-03) ⁺	9.957E-01 (5.9E-04) ⁺	9.966E-01 (4.7E-04) ⁺	9.976E-01 (5.1E-04) ⁺	9.123E-01 (4.0E-02)
	10	1.000E+00 (1.1E-06) ⁺	6.258E-01 (8.6E-02) ⁺	9.971E-01 (9.6E-04) ⁺	9.996E-01 (1.9E-04) ⁺	9.913E-01 (2.1E-02) ⁺	9.991E-01 (3.6E-04) ⁺	6.001E-01 (6.3E-02)
	15	9.996E-01 (3.1E-04) ⁺	7.126E-01 (7.3E-02) ⁺	9.913E-01 (3.9E-02) ⁺	9.995E-01 (2.5E-04) ⁺	9.984E-01 (5.8E-04) ⁺	9.996E-01 (1.6E-04) ⁺	4.646E-01 (1.5E-01)
MaF11	5	9.940E-01 (1.5E-03) ⁺	9.776E-01 (2.4E-03) ⁻	9.910E-01 (1.3E-03) ⁻	9.943E-01 (8.4E-04) ⁺	9.881E-01 (3.3E-03) ⁻	9.958E-01 (4.7E-04) ⁺	9.929E-01 (1.1E-03)
	10	9.984E-01 (8.3E-04) ⁺	9.884E-01 (2.1E-03) ⁻	9.942E-01 (8.0E-04) ⁺	9.986E-01 (6.0E-04) ⁺	9.892E-01 (2.4E-03) ⁻	9.971E-01 (1.2E-03) ⁺	9.938E-01 (1.7E-03)
	15	9.944E-01 (2.1E-03) ⁺	9.889E-01 (3.4E-03) ⁻	9.940E-01 (1.1E-03) ⁻	9.990E-01 (6.7E-04) ⁺	9.728E-01 (6.0E-03) ⁻	9.983E-01 (6.7E-04) ⁺	9.921E-01 (2.7E-03)
MaF12	5	6.925E-01 (5.9E-02) ⁺	6.857E-01 (1.2E-02) ⁺	7.431E-01 (2.7E-02) ⁺	7.266E-01 (5.6E-03) ⁺	7.375E-01 (7.2E-03) ⁺	7.223E-01 (1.4E-02) ⁺	6.588E-01 (5.4E-02)
	10	7.992E-01 (6.5E-02) ⁺	8.183E-01 (1.1E-02) ⁺	8.908E-01 (6.2E-02) ⁺	8.725E-01 (7.8E-03) ⁺	8.759E-01 (3.3E-02) ⁺	8.546E-01 (5.8E-02) ⁺	7.634E-01 (5.5E-02)
	15	7.172E-01 (5.9E-02) ⁻	8.519E-01 (1.1E-02) ⁺	9.316E-01 (3.6E-02) ⁺	9.300E-01 (5.3E-03) ⁺	8.552E-01 (5.3E-02) ⁺	8.658E-01 (5.2E-02) ⁺	7.629E-01 (5.4E-02)
MaF13	5	2.347E-01 (1.1E-02) ⁻	2.835E-01 (5.3E-03) ⁺	2.056E-01 (1.2E-02) ⁻	1.967E-01 (2.0E-02) ⁻	1.577E-01 (1.6E-02) ⁻	1.899E-01 (1.8E-02) ⁻	2.504E-01 (2.5E-02)
	10	1.215E-01 (4.6E-03) ⁺	1.381E-01 (1.9E-03) ⁺	1.072E-01 (1.1E-02) ⁻	1.130E-02 (2.9E-02) ⁻	8.907E-02 (1.8E-02) ⁻	1.131E-01 (1.0E-02) ⁻	1.153E-01 (2.2E-02)
	15	7.421E-02 (6.6E-03) ⁻	8.958E-02 (2.0E-03) ⁺	7.191E-02 (8.9E-03) ⁻	3.880E-02 (2.6E-02) ⁻	5.270E-02 (2.0E-02) ⁻	6.938E-02 (1.6E-02) ⁻	7.940E-02 (2.0E-02)
MaF14	5	5.492E-01 (6.1E-02) ⁻	6.228E-01 (5.9E-02) ⁻	4.099E-01 (1.2E-01) ⁻	2.938E-01 (2.2E-01) ⁻	2.817E-01 (2.0E-01) ⁻	3.228E-01 (1.7E-01) ⁻	6.619E-01 (1.3E-01)
	10	4.089E-01 (1.5E-01) ⁻	1.192E-01 (1.3E-01) ⁻	0.000E+00 (0.0E+00) ⁻	1.027E-02 (3.0E-02) ⁻	6.055E-01 (1.1E-01) ⁺	1.749E-02 (4.4E-02) ⁻	4.653E-01 (2.5E-01)
	15	1.189E-01 (1.2E-01) ⁻	6.581E-04 (1.9E-03) ⁻	0.000E+00 (0.0E+00) ⁻	3.734E-01 (2.9E-01) ⁺	2.931E-01 (2.1E-01) ⁻	1.656E-02 (3.5E-02) ⁻	3.560E-01 (2.2E-01)
MaF15	5	1.675E-05 (5.2E-05) ⁻	5.796E-02 (1.2E-02) ⁺	1.139E-07 (6.3E-07) ⁻	1.395E-04 (3.7E-04) ⁻	1.592E-02 (7.5E-03) ⁻	1.145E-06 (4.4E-06) ⁻	4.009E-02 (1.0E-02)
	10	0.000E+00 (0.0E+00) ⁻	4.935E-05 (3.4E-05) ⁺	0.000E+00 (0.0E+00) ⁻	1.032E-12 (3.5E-12) ⁻	1.480E-06 (9.2E-07) ⁻	0.000E+00 (0.0E+00) ⁻	5.686E-06 (4.9E-06)
	15	0.000E+00 (0.0E+00) ⁻	2.056E-13 (2.5E-13) ⁻	0.000E+00 (0.0E+00) ⁻	2.046E-20 (8.1E-20) ⁻	1.871E-12 (3.8E-12) ⁻	0.000E+00 (0.0E+00) ⁻	1.347E-10 (1.8E-10)

Wilcoxon's rank sum test at a 0.05 significance level is performed in terms of HV values. "+", "-" or "≈" indicate that the results obtained by corresponding algorithms is significantly better, worse or similar to that of MaOEA-CS on this test instance, respectively.

E. Parameter Sensitivity Studies

Two parameters, i.e., the switching threshold Δ_t and the learning period len , exist in MaOEA-CS. In this section, the sensitivity of them with regard to MaOEA-CS is investigated. In the experiments, Δ_t is set to 1.0, 0.1, 0.01, 0.001, 0.0001 or 0.00001 and len is set from 10 to 90 with the step size 20. The experiments are conducted on 10-objective MaF4 and MaF9 with a total number of 6×5 different parameter configurations. 30 independent runs have been conducted for each configuration on each test problem.

Fig. 4 shows the IGD values obtained by MaOEA-CS with 30 different combinations of Δ_t and len on 10-objective MaF4. It can be observed that, MaOEA-CS achieves the good performance in terms of IGD when the setting of learning period len positively correlates to the setting of the switching threshold Δ_t . This can be explained as follows.

In MaOEA-CS, the first search process (emphasizing ex-

plorative search) should be conducted until the corner solutions have been approximated (i.e., nadir point do not change much). After that, the second search process (emphasizing explorative search) is conducted for improving the diversity of the solution set. If the learning period len is set to a small value, the change of the nadir point also tends to be a small value. In other words, a small value of the learning period len also requires a small value of switching threshold Δ_t , and vice versa. In addition, it also can be observed from Fig. 4 that the best performance can be achieved in terms of IGD on MaF4, when $\Delta_t = 0.1$ and $len = 70$.

Fig. 5 shows the IGD values with 30 different parameters on 10-objective MaF9. Similar phenomenon can be observed that the setting of len and Δ_t should be positively correlated to achieve good performance. It also can be observed from Fig. 5 that the best performance can be achieved in terms of IGD on MaF9, when $\Delta_t = 0.1$ and $len = 30$.

TABLE IV: The ranks of all the seven compared algorithms on MaF1-15

Problem	m	HV							IGD						
		BCE-MOEA/D	GSRA	KnEA	RSEA	RVEA	NSGA-III	MaOEA-CS	BCE-MOEA/D	GSRA	KnEA	RSEA	RVEA	NSGA-III	MaOEA-CS
MaF1	5	4	5	2	3	7	6	1	4	3	2	5	7	6	1
	10	2	5	3	1	7	6	4	5	4	2	3	7	6	1
	15	3	5	5	1	4	2	5	6	6	4	2	3	7	5
MaF2	5	5	1	2	4	7	6	3	2	3	6	4	5	7	1
	10	5	2	6	1	7	4	3	3	2	1	6	7	4	5
	15	5	3	6	1	7	4	2	3	2	1	5	7	4	6
MaF3	5	6	5	7	3	4	2	1	6	1	7	2	3	4	5
	10	4	2	7	5	3	6	1	4	1	7	5	3	6	2
	15	4	2	6	6	3	5	1	4	1	7	5	2	6	3
MaF4	5	6	4	1	3	7	5	2	5	3	2	4	7	6	1
	10	5	6	3	1	7	2	4	2	6	3	5	7	4	1
	15	4	5	3	1	6	2	7	4	6	3	2	7	5	1
MaF5	5	3	7	2	6	4	5	1	2	3	5	6	4	7	1
	10	6	7	2	5	4	1	3	6	2	3	4	7	5	1
	15	7	6	1	4	5	2	3	6	2	3	4	7	5	1
MaF6	5	2	4	3	5	7	6	1	2	4	3	7	6	5	1
	10	2	6	6	4	3	5	1	1	5	7	4	3	6	2
	15	2	6	6	5	3	4	1	2	5	7	4	3	6	1
MaF7	5	7	4	1	2	6	5	3	3	2	1	7	6	5	4
	10	4	6	7	1	3	5	2	3	1	2	6	7	5	4
	15	5	6	7	1	3	4	2	2	1	4	7	6	5	3
MaF8	5	4	1	5	3	7	6	2	3	1	6	4	7	5	2
	10	4	3	5	1	7	6	2	1	4	3	5	7	6	2
	15	4	6	3	1	7	5	2	2	7	3	4	6	5	1
MaF9	5	3	1	7	6	5	4	2	3	1	7	6	5	4	2
	10	6	1	7	3	5	4	2	6	1	7	3	5	4	2
	15	7	1	3	4	6	5	2	6	1	4	3	7	5	2
MaF10	5	2	7	5	4	3	1	6	3	7	4	5	1	2	6
	10	1	6	4	2	5	3	7	5	6	2	3	4	1	7
	15	2	6	5	3	4	1	7	3	6	2	4	5	1	7
MaF11	5	3	7	5	2	6	1	4	1	7	2	3	6	4	5
	10	2	7	4	1	6	3	5	1	7	3	2	6	5	4
	15	3	6	4	1	7	2	5	2	6	4	3	7	5	1
MaF12	5	5	6	1	3	2	4	7	6	5	4	7	3	2	1
	10	6	5	1	3	2	4	7	4	2	5	7	3	6	1
	15	7	5	1	2	4	3	6	3	5	2	7	4	6	1
MaF13	5	3	1	4	5	7	6	2	2	1	3	4	7	5	6
	10	2	1	5	7	6	4	3	2	1	3	5	6	4	7
	15	3	1	4	7	6	5	2	2	1	3	5	6	4	7
MaF14	5	3	2	4	6	7	5	1	3	2	4	5	7	6	1
	10	3	4	7	6	1	5	2	3	4	7	5	1	6	2
	15	4	6	7	1	3	5	2	4	6	7	3	1	5	2
MaF15	5	5	1	7	4	3	6	2	5	1	7	4	3	6	2
	10	5	1	5	4	3	5	2	6	1	7	4	3	5	2
	15	5	3	5	4	2	5	1	5	1	7	4	3	6	2
Mean Rank		4.07	4.11	4.31	3.24	4.91	4.11	2.98	3.47	3.22	4.09	4.51	5.13	4.89	2.69
Total Rank		3	4	6	2	7	4	1	3	2	4	5	7	6	1

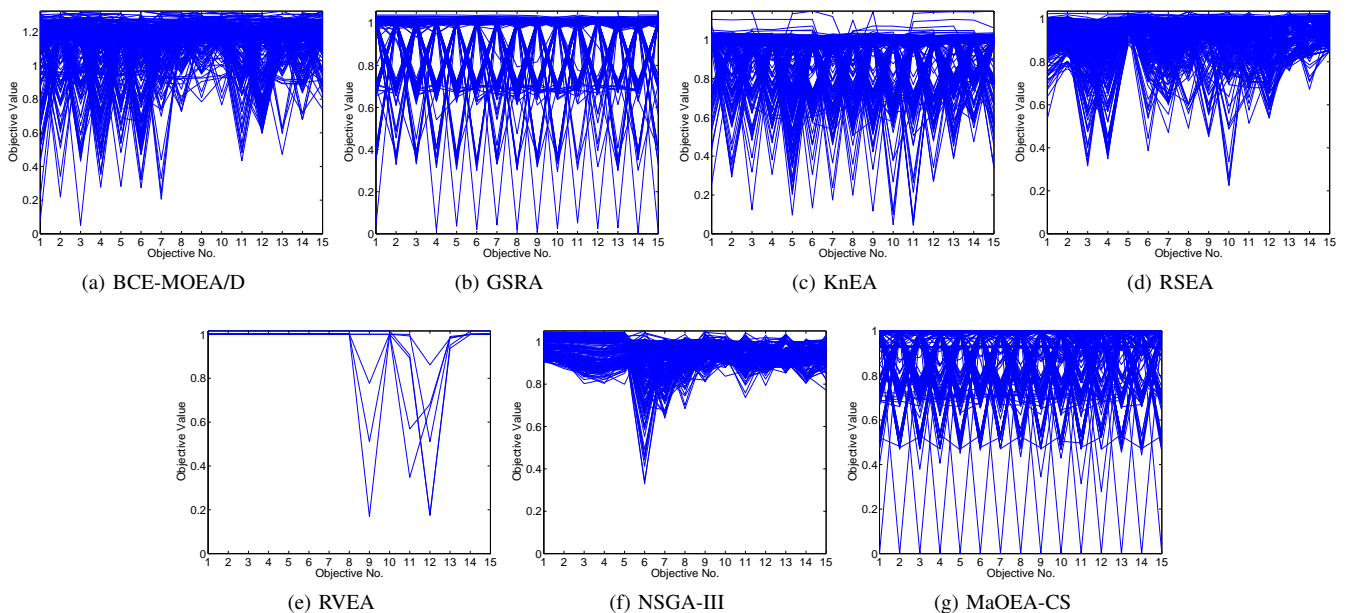


Fig. 3: The parallel coordinates plots of the nondominated sets obtained by seven compared algorithms, in the run with the median IGD values on 15-objective MaF1.

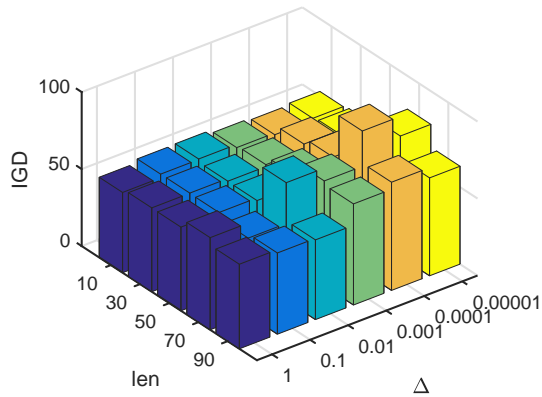


Fig. 4: Mean IGD values obtained by MaOEA-CS with 30 different combinations of Δ_t and len on 10-objective MaF4

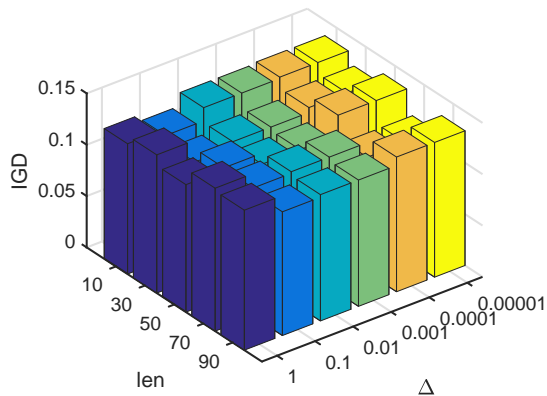


Fig. 5: Mean IGD values obtained by MaOEA-CS with 30 different combinations of Δ_t and len on 10-objective MaF9

V. APPLICATIONS ON THE REAL-WORLD OPTIMIZATION PROBLEMS

In this section, MaOEA-CS is applied and compared with other six algorithms on two real-world engineering optimization problems.

- 1) Crash-worthiness design of vehicles (CWDV) can be formulated as the structural optimization on the frontal structure of vehicle for crash-worthiness [60]. Thickness of five reinforced members around the frontal structure are chosen as the design variables, while mass of vehicle, deceleration during the full frontal crash and toe board intrusion in the offset-frontal crash are considered as three objectives. More detailed mathematical formulation can be found in [60].
- 2) Car side-impact problem (CSIP) aims at finding a design that balances between the weight and the safety performance. It is firstly formulated for the minimization of the weight of the car subject to some safety restrictions on safety performance [61], [62]. In [62], it is reformulated as a 9-objective optimization problem by treating some constraints as objectives. More details of the mathematical formulation can be found in [62].

A. Experimental setups

For CWDV, the population size is set to 120; and the maximum number of allowed iterations is set to 200. For CSIP, The population size are set to 210; and the maximum number of iterations is set to 2000. All the seven compared algorithms are run for 30 times on each problem. Other parameters in all the compared algorithm are set the same as that in Section. IV-B.

As the real PFs of both CWDV and CSIP are unknown, to compute IGD, a reference PF (denoted as P^*) is constructed by obtaining all the nondominated solutions of all 30 runs obtained by all the compared algorithms for each problem. To compute HV, each objective value of all the nondominated solutions are firstly normalized to $[0, 1]$ by the maximal and minimal values of P^* ; and the reference point is set to $(1.1, \dots, 1.1)^T$.

B. Experimental results

The performance of all the seven compared algorithms, in terms of IGD and HV, are given in Table V. For CWDV, MaOEA-CS obtains the best performance in terms of both IGD and HV. To visualize the performance of all the compared algorithms, the nondominated solutions obtained by all the seven algorithms in the run with the median IGD values are plotted in Fig. 6. It can be observed that CWDV has a discontinuous PF and only MaOEA-CS can obtain the nondominated solutions on all parts of PFs.

As for CSIP, MaOEA-CS has the best performance in terms of HV while BCE-MOEA/D has the best performance in terms of IGD. To further visualize the performance of all the compared algorithms, the parallel coordinate plots of all the nondominated solutions obtained by the seven algorithms over 30 runs are illustrated in Fig. 7. A reference PF is approximated by using all the nondominated solutions obtained by all the seven algorithms over 30 runs, as shown in Fig. 7h. It can be observed that only MaoEA-CS is able to obtain solutions with the minimum objective values on all the objectives. This can be explained by the fact that MaOEA-CS is able to locate the boundary of PFs by the approximation of the corner solutions. This also explains why MaOEA-CS can achieve better performance in terms of HV.

In addition, it also can be observed in Fig. 7a and Fig. 3c that BCE-MOEA/D and KnEA are able to obtain more diversely-populated solutions inside the PF boundaries. As IGD indicator may prefer solutions located inside the PF boundaries, BCE-MOEA/D and KnEA achieves better performance in terms of IGD on CSIP.

All the above experimental studies indicate that MaoEA-CS has satisfactory performance on the real-world optimization problems which usually have very irregular PFs.

VI. CONCLUSION

In this paper, a many-objective evolutionary algorithm based on corner solution search was proposed and compared with six state-of-the-art algorithms on MaF test suite with various different characteristics for CEC'2017 MaOEA Competition.

TABLE V: Experimental results of 7 algorithms on CWDV and CSIP

Problem	indicator	BCE-MOEA/D	GSRA	KnEA	RSEA	RVEA	NSGA-III	MaOEA-CS
CWDV	IGD	3.342e-02 (4.4e-04) ⁻	1.780e-01 (1.2e-04) ⁻	5.192e-02 (4.9e-03) ⁻	3.466e-02 (8.0e-04) ⁻	6.134e-02 (1.3e-02) ⁻	3.822e-02 (3.0e-03) ⁻	1.831e-02 (6.8e-04)
	HV	9.800e-01 (3.0e-03) ⁻	9.251e-01 (1.1e-03) ⁻	9.676e-01 (4.7e-03) ⁻	9.770e-01 (3.2e-03) ⁻	9.533e-01 (1.3e-02) ⁻	9.765e-01 (2.7e-03) ⁻	1.017e+00 (1.0e-03)
CSIP	IGD	1.761e-01 (3.4e-03) ⁺	3.105e-01 (1.5e-02) ⁻	1.909e-01 (1.6e-02) ⁺	3.008e-01 (5.0e-02) ⁻	3.444e-01 (1.9e-02) ⁻	1.955e-01 (6.7e-03) ⁻	1.937e-01 (1.0e-02)
	HV	1.653e-01 (1.0e-02) ⁻	1.182e-01 (1.7e-02) ⁻	1.609e-01 (1.6e-02) ⁻	2.196e-01 (1.0e-02) ⁻	8.066e-02 (1.9e-02) ⁻	1.533e-01 (1.7e-02) ⁻	2.569e-01 (1.0e-02)

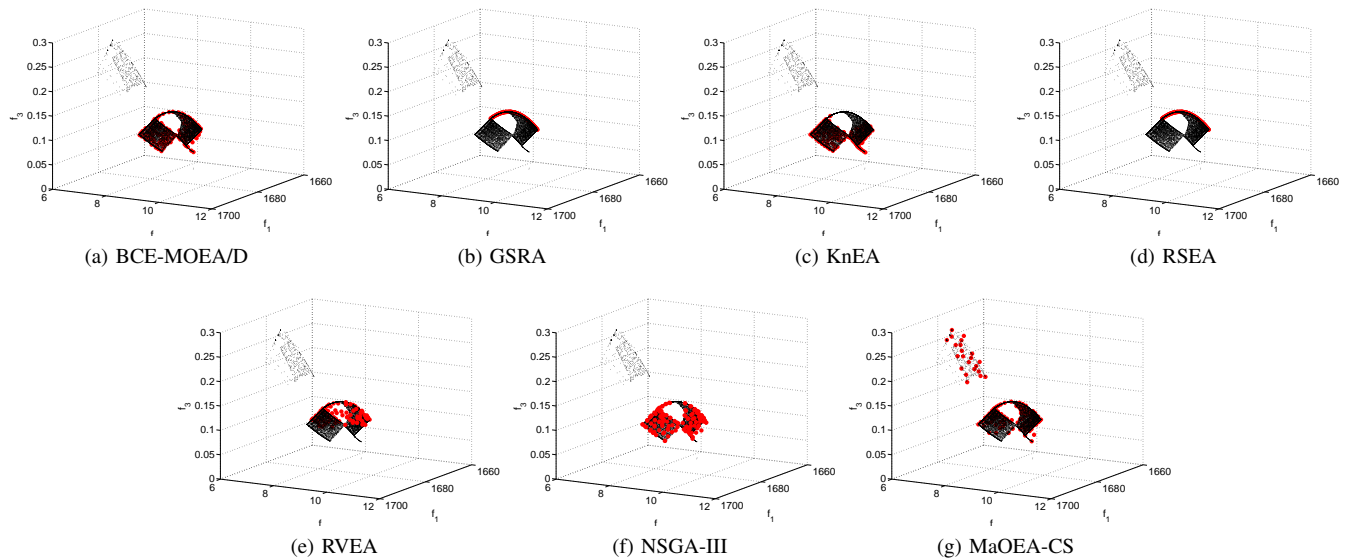


Fig. 6: The nondominated solutions obtained by all the seven compared algorithms on CWDV (marked by red circle), the small black dots represent PF approximations obtained by all the seven compared algorithms over all 30 runs.

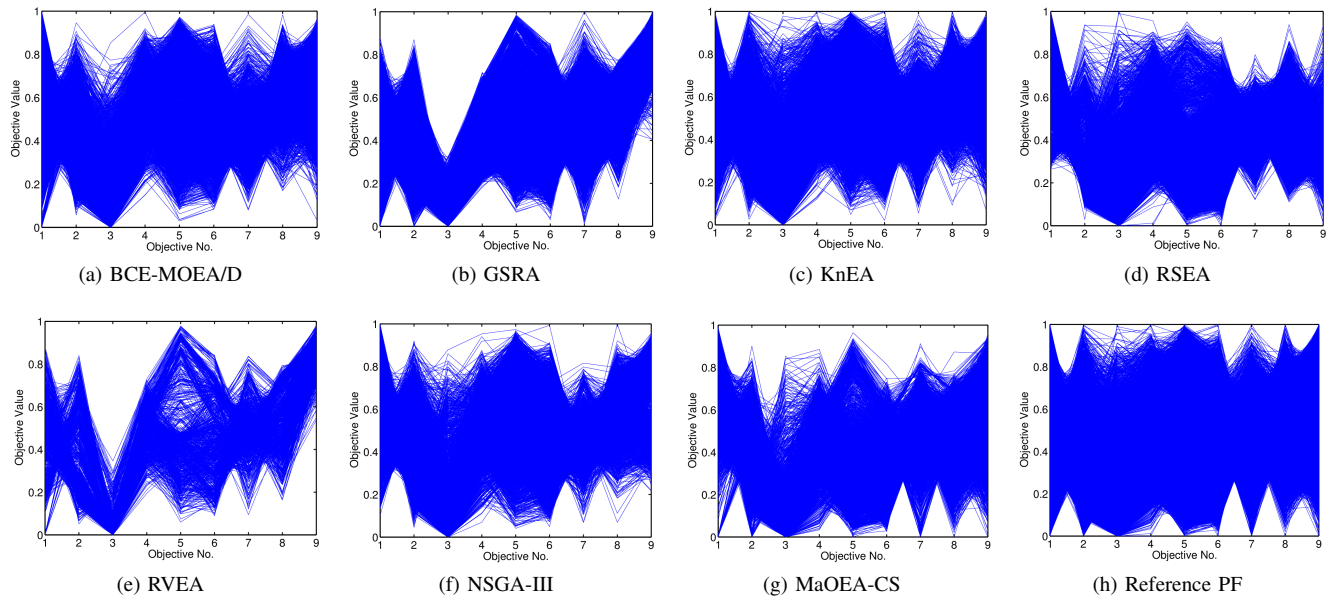


Fig. 7: The parallel coordinate plots of all the non-dominated solutions obtained by seven compared algorithms on CSIP over 30 runs. Among them, Fig. 7h presents the parallel coordinate plots of reference PF approximations obtained by all the seven compared algorithms over 30 runs.

The experimental results show that the proposed MaOEA-CS has the best overall performance. This indicates MaOEA-CS is more robust than other compared algorithms on various test problems thus it successfully won the CEC'2017 MaOEA Competition. The sensitivity test of two parameters in MaOEA-CS were also conducted and analyzed in this paper. In addition, MaOEA-CS has also been applied on two real-world engineering optimization problems with very irregular PFs. The experimental results show that MaOEA-CS outperforms other six compared algorithms in terms of either convergence or diversity, which indicates it has the ability to handle real-world complex optimization problems with irregular PFs.

REFERENCES

- [1] X. Cai, Z. Yang, Z. Fan, and Q. Zhang, "Decomposition-based-sorting and angle-based-selection for evolutionary multiobjective and many-objective optimization," *IEEE Transactions on Cybernetics*, in press, 2017.
- [2] K. Miettinen, *Nonlinear Multiobjective Optimization*. Boston: Kluwer Academic Publishers, 1999.
- [3] C. A. C. Coello, *Evolutionary multi-objective optimization: a historical view of the field*. IEEE Press, 2006.
- [4] C. A. C. Coello, "20 years of evolutionary multi-objective optimization: What has been done and what remains to be done," 2006.
- [5] K. Deb, A. Pratap, S. Agarwal, and T. Meyarivan, "A fast and elitist multiobjective genetic algorithm: Nsga-ii," *IEEE Transactions on Evolutionary Computation*, vol. 6, no. 2, pp. 182–197, 2002.
- [6] Q. Zhang and H. Li, "MOEA/D: A multiobjective evolutionary algorithm based on decomposition," *IEEE Transactions on Evolutionary Computation*, vol. 11, no. 6, pp. 712–731, 2007.
- [7] K. Deb and D. Kalyanmoy, *Multi-Objective Optimization Using Evolutionary Algorithms*. John Wiley & Sons, 2001.
- [8] C. M. Fonseca and P. J. Fleming, "An overview of evolutionary algorithms in multiobjective optimization," *Evolutionary Computation*, vol. 3, no. 1, pp. 1–16, 2014.
- [9] H. Ishibuchi, N. Tsukamoto, and Y. Nojima, "Evolutionary many-objective optimization: A short review," in *Evolutionary Computation, 2008. CEC 2008. (IEEE World Congress on Computational Intelligence). IEEE Congress on*, pp. 2419–2426, IEEE, 2008.
- [10] B. Li, J. Li, K. Tang, and X. Yao, "Many-objective evolutionary algorithms: A survey," *ACM Computing Surveys (CSUR)*, vol. 48, no. 1, p. 13, 2015.
- [11] C. M. Fonseca and P. J. Fleming, "Multiobjective optimization and multiple constraint handling with evolutionary algorithms—Part I: A unified formulation," *IEEE Transactions on Systems, Man, and Cybernetics, Part A: Systems and Humans*, vol. 28, no. 1, pp. 26–37, 1998.
- [12] R. C. Purshouse and P. J. Fleming, "On the evolutionary optimization of many conflicting objectives," *IEEE Transactions on Evolutionary Computation*, vol. 11, no. 6, pp. 770–784, 2007.
- [13] J. Knowles and D. Corne, "Quantifying the effects of objective space dimension in evolutionary multiobjective optimization," in *International Conference on Evolutionary Multi-Criterion Optimization*, pp. 757–771, Springer, 2007.
- [14] D. W. Corne and J. D. Knowles, "Techniques for highly multiobjective optimisation: some nondominated points are better than others," *Proceedings of International Conference on Genetic and Evolutionary Computation*, pp. 773–780, 2007.
- [15] E. Zitzler, M. Laumanns, and L. Thiele, "Spea2: Improving the strength pareto evolutionary algorithm," 2001.
- [16] H. Ishibuchi, N. Akedo, and Y. Nojima, "Behavior of multiobjective evolutionary algorithms on many-objective knapsack problems," *IEEE Transactions on Evolutionary Computation*, vol. 19, no. 2, pp. 264–283, 2015.
- [17] Y. Jin and B. Sendhoff, "Connectedness, regularity and the success of local search in evolutionary multi-objective optimization," in *Evolutionary Computation, 2003. CEC'03. The 2003 Congress on*, vol. 3, pp. 1910–1917, IEEE, 2003.
- [18] J. Bader and E. Zitzler, "Hype: an algorithm for fast hypervolume-based many-objective optimization," *Evolutionary Computation*, vol. 19, no. 1, p. 45, 2011.
- [19] K. Li, K. Deb, Q. Zhang, and S. Kwong, "An evolutionary many-objective optimization algorithm based on dominance and decomposition," *IEEE Transactions on Evolutionary Computation*, vol. 19, no. 5, pp. 694–716, 2015.
- [20] Z. He and G. G. Yen, "Many-objective evolutionary algorithm: Objective space reduction and diversity improvement," *IEEE Transactions on Evolutionary Computation*, vol. 20, no. 1, pp. 145–160, 2016.
- [21] H. Wang, L. Jiao, and X. Yao, "Two_arch2: An improved two-archive algorithm for many-objective optimization," *IEEE Transactions on Evolutionary Computation*, vol. 19, no. 4, pp. 524–541, 2015.
- [22] S. Yang, M. Li, X. Liu, and J. Zheng, "A grid-based evolutionary algorithm for many-objective optimization," *IEEE Transactions on Evolutionary Computation*, vol. 17, no. 5, pp. 721–736, 2013.
- [23] X. Zhang, Y. Tian, and Y. Jin, "A knee point-driven evolutionary algorithm for many-objective optimization," *IEEE Transactions on Evolutionary Computation*, vol. 19, no. 6, pp. 761–776, 2015.
- [24] R. Cheng, Y. Jin, M. Olhofer, and B. Sendhoff, "A reference vector guided evolutionary algorithm for many-objective optimization," *IEEE Transactions on Evolutionary Computation*, vol. 20, 2016.
- [25] K. Deb and H. Jain, "An evolutionary many-objective optimization algorithm using reference-point-based nondominated sorting approach, part i: Solving problems with box constraints," *IEEE Transactions on Evolutionary Computation*, vol. 18, no. 4, pp. 577–601, 2014.
- [26] M. Laumanns, L. Thiele, K. Deb, and E. Zitzler, "Combining convergence and diversity in evolutionary multiobjective optimization," *Evolutionary Computation*, vol. 10, no. 3, pp. 263–282, 2002.
- [27] D. Hadka and P. Reed, *Borg: An Auto-Adaptive Many-Objective Evolutionary Computing Framework*. MIT Press, 2013.
- [28] S. Yang, M. Li, X. Liu, and J. Zheng, "A grid-based evolutionary algorithm for many-objective optimization," *Evolutionary Computation, IEEE Transactions on*, vol. 17, no. 5, pp. 721–736, 2013.
- [29] K. Le, D. Landa-Silva, and H. Li, *An Improved Version of Volume Dominance for Multi-Objective Optimisation*. Springer Berlin Heidelberg, 2009.
- [30] H. Aguirre, A. Oyama, and K. Tanaka, *Adaptive ϵ -Sampling and ϵ -Hood for Evolutionary Many-Objective Optimization*. Springer Berlin Heidelberg, 2013.
- [31] H. Aguirre and K. Tanaka, "A hybrid scalarization and adaptive ϵ -ranking strategy for many-objective optimization," *Field Analytical Chemistry & Technology*, vol. 1, no. 6, p. 367374, 2010.
- [32] S. F. Adra and P. J. Fleming, "Diversity management in evolutionary many-objective optimization," *Evolutionary Computation, IEEE Transactions on*, vol. 15, no. 2, pp. 183–195, 2011.
- [33] M. Li, S. Yang, and X. Liu, "Shift-based density estimation for pareto-based algorithms in many-objective optimization," *Evolutionary Computation, IEEE Transactions on*, vol. 18, no. 3, pp. 348–365, 2014.
- [34] E. Zitzler and L. Thiele, "Multiobjective Evolutionary Algorithms: A Comparative Case Study and the Strength Pareto Approach," *IEEE Transactions on Evolutionary Computation*, vol. 3, pp. 257–271, November 1999.
- [35] M. T. Emmerich, *Single- and Multi-objective Evolutionary Design Optimization Assisted by Gaussian Random Field Metamodels*. PhD thesis, University of Dortmund, Germany, October 2005.
- [36] H. Ishibuchi, Y. Sakane, N. Tsukamoto, and Y. Nojima, "Evolutionary many-objective optimization by nsga-ii and moea/d with large populations," in *Systems, Man and Cybernetics, 2009. SMC 2009. IEEE International Conference on*, pp. 1758–1763, IEEE, 2009.
- [37] H. Ishibuchi, S. Yu, H. Masuda, and Y. Nojima, "Performance of decomposition-based many-objective algorithms strongly depends on pareto front shapes," *IEEE Transactions on Evolutionary Computation*, vol. PP, no. 99, pp. 1–1, 2016.
- [38] X. Cai, Z. Mei, and Z. Fan, "A decomposition-based many-objective evolutionary algorithm with two types of adjustments for direction vectors," *IEEE Transactions on Cybernetics*, vol. PP, no. 99, pp. 1–14, 2017.
- [39] H. K. Singh, A. Isaacs, and T. Ray, "A pareto corner search evolutionary algorithm and dimensionality reduction in many-objective optimization problems," *IEEE Transactions on Evolutionary Computation*, vol. 15, no. 4, pp. 539–556, 2011.
- [40] D. Gong, G. Wang, and X. Sun, "Set-based genetic algorithms for solving many-objective optimization problems," in *Computational Intelligence*, pp. 96–103, 2013.
- [41] H. Jain and K. Deb, "An evolutionary many-objective optimization algorithm using reference-point based nondominated sorting approach, part ii: Handling constraints and extending to an adaptive approach," *IEEE Transactions on Evolutionary Computation*, vol. 18, no. 4, pp. 602–622, 2014.

- [42] R. Cheng, M. Li, Y. Tian, X. Zhang, S. Yang, Y. Jin, and X. Yao, "A benchmark test suite for evolutionary many-objective optimization," *Complex&Intelligence Systems*, vol. 3, no. 1, pp. 67–81, 2017.
- [43] X. Cai, Y. Li, Z. Fan, and Q. Zhang, "An external archive guided multiobjective evolutionary algorithm based on decomposition for combinatorial optimization," *Evolutionary Computation IEEE Transactions on*, vol. 19, no. 4, pp. 508–523, 2015.
- [44] X. Cai, Z. Yang, Z. Fan, and Q. Zhang, "Decomposition-based-sorting and angle-based-selection for evolutionary multiobjective and many-objective optimization," *IEEE transactions on cybernetics*, 2016.
- [45] X. Cai, Z. Mei, Z. Fan, and Q. Zhang, "A constrained decomposition approach with grids for evolutionary multiobjective optimization," *IEEE Transactions on Evolutionary Computation*, vol. PP, no. 99, pp. 1–1, 2017.
- [46] K. Deb and R. B. Agrawal, "Simulated binary crossover for continuous search space," *Complex Systems*, vol. 9, no. 3, pp. 115–148, 1994.
- [47] K. Deb and M. Goyal, "A combined genetic adaptive search for engineering design," in *International Conference on Genetic Algorithms*, pp. 30–45, 1999.
- [48] H. L. Liu, F. Gu, and Q. Zhang, "Decomposition of a multiobjective optimization problem into a number of simple multiobjective subproblems," *IEEE Transactions on Evolutionary Computation*, vol. 18, no. 3, pp. 450–455, 2014.
- [49] H. L. Liu and X. Li, "The multiobjective evolutionary algorithm based on determined weight and sub-regional search," in *Evolutionary Computation, 2009. CEC '09. IEEE Congress on*, pp. 1928–1934, 2009.
- [50] Q. Zhang, W. Liu, and H. Li, "The performance of a new version of MOEA/D on CEC09 unconstrained mop test instances," Working Report CES-491, School of CS and EE, University of Essex, February 2009.
- [51] M. Li, S. Yang, and X. Liu, "Pareto or non-pareto: Bi-criterion evolution in multiobjective optimization," *IEEE Transactions on Evolutionary Computation*, vol. 20, no. 5, pp. 645–665, 2016.
- [52] H. S. P. J. Ye chen, Xiaoping Yuan, "Gradient stochastic ranking-based multi-indicator algorithm." Website, 2017. <https://github.com/ranchengcn/IEEE-CEC-MaOO-Competition/blob/master/2017/Source%20code%20of%20entries/GSRA.pdf>.
- [53] C. He, Y. Tian, Y. Jin, X. Zhang, and L. Pan, "A radial space division based evolutionary algorithm for many-objective optimization," *Applied Soft Computing*, vol. 61, 2017.
- [54] Y. Tian, R. Cheng, X. Zhang, and Y. Jin, "Platemo: A matlab platform for evolutionary multi-objective optimization," 2017.
- [55] M. R. Sierra and C. A. Coello, "A new multi-objective particle swarm optimizer with improved selection and diversity mechanisms," 2004.
- [56] C. A. C. Coello and M. R. Sierra, "A study of the parallelization of a coevolutionary multi-objective evolutionary algorithm," in *Mexican International Conference on Artificial Intelligence*, pp. 688–697, 2004.
- [57] A. Zhou, Q. Zhang, Y. Jin, E. P. K. Tsang, and T. Okabe, "A model-based evolutionary algorithm for bi-objective optimization," in *Proceedings of the IEEE Congress on Evolutionary Computation, CEC 2005, 2-4 September 2005, Edinburgh, UK*, pp. 2568–2575, 2005.
- [58] L. While, P. Hingston, L. Barone, and S. Huband, "A faster algorithm for calculating hypervolume," *IEEE Transactions on Evolutionary Computation*, vol. 10, no. 1, pp. 29–38, 2006.
- [59] A. Inselberg, *Parallel Coordinates: Visual Multidimensional Geometry and Its Applications*. New York, NY, USA: Springer, 2009.
- [60] X. Liao, Q. Li, X. Yang, W. Zhang, and W. Li, "Multi-objective optimization for crash safety design of vehicles using stepwise regression model," *Chinese Journal of Mechanical Engineering*, vol. 35, no. 6, pp. 561–569, 2007.
- [61] L. Gu, R. J. Yang, C. H. Tho, M. Makowskit, O. Faruquet, and YLi, "Optimisation and robustness for crashworthiness of side impact," *International Journal of Vehicle Design*, vol. 26, no. 4, pp. 348–360(13), 2001.
- [62] K. Deb, S. Gupta, D. Daum, J. Branke, rgen, A. K. Mall, and D. Padmanabhan, "Reliability-based optimization using evolutionary algorithms," *IEEE Transactions on Evolutionary Computation*, vol. 13, no. 5, pp. 1054–1074, 2009.